

Original Article

Comparative metabolome analysis of cultured fetal and adult hepatocytes in humans

Su-Ryang Kim¹, Takashi Kubo^{1,4}, Yukie Kuroda¹, Maki Hojo¹, Takuya Matsuo²,
Atsuko Miyajima³, Makoto Usami¹, Yuko Sekino¹, Taku Matsushita² and Seiichi Ishida¹

¹Division of Pharmacology, National Institute of Health Sciences, 1-18-1 Kamiyoga, Setagaya-ku, Tokyo 158-8501, Japan

²Faculty of Biotechnology and Life Science, Sojo University, 4-22-1 Ikeda, Nishi-ku, Kumamoto 860-0082, Japan

³Division of Medical Devices, National Institute of Health Sciences, 1-18-1 Kamiyoga, Setagaya-ku, Tokyo 158-8501, Japan

⁴Present address: Division of Translational Research, Exploratory Oncology Research & Clinical Trial Center, National Cancer Center, 5-1-1 Tsukiji, Chuo-ku, Tokyo 104-0045, Japan

(Received May 19, 2014; Accepted July 6, 2014)

ABSTRACT — The liver is the central organ of metabolism, but its function varies during development from fetus to adult. In this study, we comprehensively analyzed and compared metabolites in fetal and adult hepatocytes, the major parenchymal cell in the liver, from human donors. We identified 211 metabolites (116 anions and 95 cations) by capillary electrophoresis-time-of-flight mass spectrometry (CE-TOFMS) in the hepatocytes cultured *in vitro*. Principal component analysis and hierarchical clustering analysis of the relative amounts of metabolites clearly classified hepatocytes into 2 groups that were consistent with their origin, i.e., the fetus and adult. The amounts of most metabolites in the glycolysis/glyconeogenesis pathway, tricarboxylic acid cycle and urea cycle were lower in fetal hepatocytes than in adult hepatocytes. These results suggest different susceptibility of the fetal and adult liver to toxic insults affecting energy metabolism.

Key words: Metabolome, CE-TOFMS, Human fetal hepatocytes, Human adult hepatocytes

INTRODUCTION

The liver is the central organ of human metabolism. The liver performs several complex reactions such as plasma protein synthesis, bile production, nutrient metabolism, energy metabolism, and disposal of waste products of intermediary metabolism. In addition, the liver performs detoxification of xenobiotic compounds through phase I and II biotransformation (Arias *et al.*, 2009).

Hepatocytes are the predominant cell type in the liver, accounting for approximately 70% of the mass of the adult organ. Hepatocytes, along with biliary epithelial cells, are derived from the embryonic endoderm, while stromal cells, stellate cells, Kupffer cells and blood vessels, are of mesodermal origin (Zaret, 2008; Zhao and Duncan, 2005).

The fetal liver is important for development, and its function is distinct from that of the adult liver, functioning primarily as a hematopoietic organ. Chinnici *et al.* (2014) reported that cell suspensions obtained after collagenase digestion of human fetal livers contained approximate-

ly 35% of hepatocytic/epithelial lineage cells, while the remaining cells were mainly erythroid cells. In rodents, fetal hepatocytes are glycolytic and have few mitochondria, suggesting that their energy production is lower than that of adult hepatocytes (Burch *et al.*, 1963; Oliver *et al.*, 1983; Vergonet *et al.*, 1970). A comparison of metabolic function between rat fetal and adult hepatocytes revealed lower activity of key metabolic enzymes in the fetal hepatocytes, including phosphoenolpyruvate carboxykinase and glucose 6-phosphatase for gluconeogenesis, carnitine palmitoyltransferase I and medium-chain acyl-CoA dehydrogenase for fatty acid oxidation, and cytochrome c and β -ATP synthase for mitochondrial energy metabolism (Sharma *et al.*, 2008).

It is also known that the expression of liver-specific genes changes transcriptionally and post-transcriptionally during rat development (Panduro *et al.*, 1987). In humans, several cytochrome P450 enzymes such as CYP1A1, 1A2, 2A6, 2C9, 2E1, and 3A4 were expressed in adult livers, whereas fewer forms of cytochrome P450, namely CYP1A1 and 3A7, were detected in fetal livers

Correspondence: Seiichi Ishida (E-mail: ishida@nihs.go.jp)

(Shimada *et al.*, 1996).

In recent years, comprehensive transcriptome analysis of rat liver and primary cultured hepatocytes treated with several chemicals was carried out and the gene expression database was used for identification of predictive biomarkers for drug-induced toxicity at or before the pre-clinical stage of drug development (Uehara *et al.*, 2010).

The metabolome is the complete set of small molecules (metabolites) in cells in a particular physiological condition and considered to be closely related to the phenotype. Thus, metabolome analysis plays a critical role in understanding complex biochemical and biological systems (Delneri *et al.*, 2001).

Recently, metabolome analysis using capillary electrophoresis-mass spectrometry (CE-MS) has been developed (Monton and Soga, 2007) and applied to the characterization of ionic metabolites from several diseases, including cancer (Hirayama *et al.*, 2009; Kami *et al.*, 2013).

Global metabolome analysis of liver has been performed in several animal models. The differences of metabolic profile in an alcoholic fatty liver in zebrafish were analyzed by proton nuclear magnetic resonance spectroscopy and gas chromatography-mass spectrometry (GC-MS) (Jang *et al.*, 2012). Metabolome profile alterations in fatty liver induced by a high-fat diet in rats were analyzed by GC-MS (Xie *et al.*, 2010). The metabolic profile changes in the liver were also analyzed in aging mice (Houtkooper *et al.*, 2011) and undernourished neonate mice (Preidis *et al.*, 2014). In humans, metabolic profiling and systems biological approaches were used to elucidate the mechanisms of metabolic syndrome and fatty liver disease (Dumas *et al.*, 2014). However, metabolome analysis of prenatal or neonatal human liver has not been investigated.

In this study, to clarify the differences of the basal metabolic functions along with the development of the liver, *in vitro* cultured human fetal and adult hepatocytes were compared by metabolome analysis using capillary electrophoresis time-of-flight mass spectrometry (CE-TOFMS).

MATERIALS AND METHODS

Cells and culture conditions

Human fetal hepatocytes (Hc cells, CS-ABI-3716) were purchased from DS Pharma Biomedical (Osaka, Japan). Hc cells were originally prepared from six normal fetal livers (gestation average 16 weeks) by Applied Cell Biology Research Institute (Kirkland, WA, USA). The cells were maintained in CS-C medium kit R (DS Pharma Biomedical) as described previously (Matsushita *et al.*, 2003). The Hc cells were divided into three aliquots that

were cultured separately.

Primary human hepatocytes (HEP220) from three adult donors were purchased from Biopredic International (Rennes, France). The primary human hepatocytes were obtained from patients undergoing resection for primary or secondary tumors, and isolated by collagenase perfusion of histologically normal liver fragment. Patient information is listed in Supplementary Table S1. The cells were maintained in Incubation Medium (MIL214; Biopredic International).

Metabolite extraction

Ionic metabolites were extracted from 2-3 × 10⁶ cells of human fetal and adult hepatocytes. Cells were washed twice with 5% mannitol solution and suspended in 1 mL of cold methanol containing 10 μM internal standards (Human Metabolome Technologies, Inc., Yamagata, Japan). The number of cells in the same culture condition was counted with a haemocytometer. The cell suspension diluted to 2 mL with methanol was mixed with 2 mL of chloroform and 0.8 mL of Milli-Q water. After centrifugation, the separated methanol-water layer was ultrafiltered using an ultrafiltration tube (Ultrafree-MC, UFC3 LCC; Millipore Corporation, Billerica, MA, USA) with a molecular weight cut-off of 5 kDa to remove proteins. The filtrate was evaporated, dissolved in 50 μL of Milli-Q water, and analyzed using CE-TOFMS.

Measurement of ionic metabolites using the CE-TOFMS system

CE-TOFMS experiments were performed using an Agilent Capillary Electrophoresis System equipped with an Agilent 6210 Time of Flight mass spectrometer, Agilent 1100 isocratic HPLC pump, Agilent G1603A CE-MS adapter kit, and Agilent G1607A CE-ESI-MS sprayer kit (Agilent Technologies, Waldbronn, Germany).

Cationic metabolites were analyzed using a fused silica capillary i.d. 50 μm × 80 cm, with Cation Buffer Solution (Human Metabolome Technologies, Inc.) as the electrolyte. The sample was injected at a pressure of 5.0 kPa for 10 sec. The applied voltage was set at 27 kV. Electro-spray ionization-mass spectrometry (ESI-MS) was conducted in the positive ion mode, and the capillary voltage was set at 4,000 V. The spectrometer was scanned from *m/z* 50 to 1,000.

Anionic metabolites were analyzed using a fused silica capillary i.d. 50 μm × 80 cm, with Anion Buffer Solution (Human Metabolome Technologies, Inc.) as the electrolyte. The sample was injected at a pressure of 5.0 kPa for 25 sec. The applied voltage was set at 30 kV. ESI-MS was conducted in the negative ion mode, and the cap-

illary voltage was set at 3,500 V. The spectrometer was scanned from m/z 50 to 1,000. Other conditions for CE-TOFMS experiments were described previously (Soga *et al.*, 2007).

Data analysis

The raw data obtained by CE-TOFMS were processed with MasterHands software (Human Metabolome Technologies, Inc.; Sugimoto *et al.*, 2010). Peak information including m/z , migration time (MT) and area was obtained. The migration time of each sample was normalized relative to the internal standards. The resulting relative area values were further normalized based on the total number of cells. Each peak was aligned according to similar migration time on CE and the m/z value was determined by TOFMS. Metabolites in the samples were identified by comparing the migration time and m/z ratio with those of authentic standards, in which differences of ± 0.5 min and ± 10 ppm were permitted, respectively. Quantitative values of metabolites are the mean \pm S.D. for 3 replicates.

The relative quantitation data of identified metabolites were imported into GeneSpring GX software (Version 12.0; Agilent Technologies, Santa Clara, CA, USA), and subjected to principal component analysis (PCA). The relative amounts of metabolites were compared by Welch's *t*-test between fetal and adult hepatocytes, with $p < 0.05$ considered to be statistically significant. Hierarchical clustering analysis and heatmap representations were also performed with GeneSpring GX software.

RNA isolation and quantitative RT-PCR analysis

Total RNA was isolated from hepatocytes with TRIzol reagent (Invitrogen, Breda, the Netherlands), followed by purification using the RNeasy Mini Kit (QIAGEN, Hilden, Germany). The concentration and purity of RNA were measured by Nanodrop ND-1000 spectrophotometer (Nyxor Biotech, Paris, France). First-strand cDNA was prepared from 1 μ g of total RNA using the High-Capacity RNA-to-cDNA Kit (Applied Biosystems, Foster City, CA, USA) with random primers. Real-time PCR assays were performed with the ABI7900 Real Time PCR System (Applied Biosystems) using the TaqMan Gene Expression Assay for ASS1 (argininosuccinate synthase 1, Hs01597989_g1), ASL (argininosuccinate lyase, Hs00902699_m1), ARG1 (arginase, Hs00968979_m1) and OTC (ornithine transcarbamylase, Hs00166892_m1), according to the manufacturer's instructions. The relative mRNA levels were determined using calibration curves obtained from serial dilutions of the pooled

hepatocyte cDNA. Transcripts of β -actin were quantified as internal controls using TaqMan β -Actin Control Reagent (Applied Biosystems). The *t*-test was applied to the comparison of the average values of mRNA levels of urea cycle enzymes between fetal and adult hepatocytes.

RESULTS AND DISCUSSION

Metabolome analysis

We performed metabolome analysis of human fetal and adult hepatocytes using CE-TOFMS. Based on m/z values and migration times, 211 metabolites (116 anion and 95 cation) were identified (Supplementary Table S2), and visualized on a large-scale metabolome pathway map (Supplementary Fig. S1), using VANTED software (Junker *et al.*, 2006). Using the whole data set of identified metabolites, we performed a principal component analysis (PCA, Fig. 1) and a hierarchical clustering analysis (HCA, Supplementary Fig. S2) to reveal the similarities/dissimilarities of 2 groups regarding variations in metabolite amounts. From the PCA score plot, fetal and adult hepatocytes were separated in the first principal component (PC1, 47% proportion). The PCA plot indicated that the metabolomic profile of the adult hepatocytes was much more heterogeneous than that of the fetal hepatocytes (Fig. 1). This may reflect the individual differences of donor patients. Metabolites with high absolute values of factor loadings for PC1 included amino acids, glycolysis/glyconeogenesis and tricarboxylic acid (TCA) cycle intermediates, and urea cycle intermediates (data not shown). A heat map representation of HCA was per-

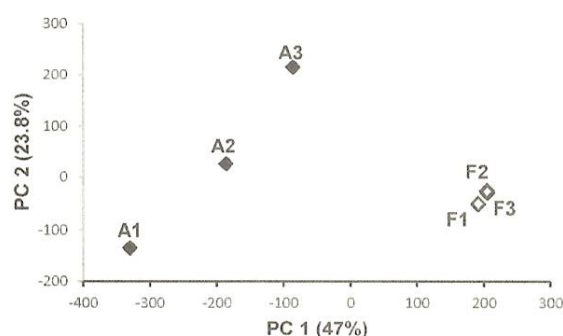


Fig. 1. PCA score plot using the normalized metabolomic data from human fetal and adult hepatocytes. The samples were fetal (F1 to F3, open diamonds) and adult (A1 to A3, filled diamonds) hepatocytes. Percentage values indicated on the axes represent the contribution rate of the first (PC1) and the second (PC2) principal components.

Table 1. Highly increased or decreased metabolites in the adult hepatocytes compared to those in the fetal hepatocytes

Compound name	Relative area ^a				Fold change (Adult/Fetal)	
	Fetal hepatocytes		Adult hepatocytes		Ratio	P value ^b
	Mean	S.D.	Mean	S.D.		
<i>increased</i>						
Cys	4.3E-04	1.6E-04	2.9E-02	1.1E-02	66.3	0.050
Ornithine	4.2E-03	1.1E-03	2.5E-01	1.1E-01	59.8	0.057
Cysteine glutathione disulphide	6.3E-04	1.3E-04	2.9E-02	2.1E-02	46.1	0.139
Thiaproline	1.9E-03	1.7E-04	6.6E-02	2.6E-02	34.6	0.050
Glycerophosphocholine	5.6E-02	9.8E-03	1.1E+00	1.0E+00	20.6	0.203
O-Phosphoserine	2.1E-04	4.3E-05	4.1E-03	1.3E-03	19.1	0.038
Glycerol 3-phosphate	4.3E-03	3.4E-04	7.5E-02	4.2E-02	17.7	0.098
Urea	1.8E-02	2.3E-03	2.0E-01	1.1E-01	11.1	0.111
Ala	2.4E-01	6.1E-03	2.3E+00	1.2E+00	9.4	0.102
Glucuronic acid	2.9E-04	2.1E-05	2.6E-03	1.7E-03	9.1	0.138
2-Hydroxybutyric acid	3.7E-04	1.1E-04	3.1E-03	2.4E-03	8.4	0.184
3-Hydroxybutyric acid	2.5E-03	3.3E-04	2.1E-02	1.6E-02	8.3	0.189
Guanidoacetic acid	1.5E-03	1.6E-04	1.2E-02	5.1E-03	8.1	0.069
N-Acetylneuraminic acid	1.4E-03	1.1E-04	1.1E-02	9.8E-03	8.0	0.235
Thiamine	1.0E-03	1.7E-04	8.2E-03	3.7E-03	7.8	0.078
Uric acid	1.3E-04	1.9E-05	9.2E-04	7.3E-04	7.2	0.201
Pyridoxamine 5'-phosphate	5.1E-04	5.7E-05	3.7E-03	1.8E-03	7.1	0.094
N ⁸ -Acetylspermidine	2.5E-03	9.5E-04	1.8E-02	6.4E-03	7.1	0.051
Citrulline	4.3E-03	3.7E-04	2.6E-02	1.0E-02	6.1	0.062
Fumaric acid	5.5E-03	3.7E-04	3.2E-02	2.1E-02	5.8	0.166
Glucaric acid	2.3E-04	5.0E-05	1.2E-03	8.9E-04	5.2	0.200
NADP ⁺	2.2E-03	9.7E-05	1.2E-02	8.0E-03	5.2	0.181
<i>decreased</i>						
2-Amino-2-(hydroxymethyl)-1,3-propanediol	3.3E-03	2.5E-04	1.1E-03	3.8E-04	0.3	0.036
2-Oxoisovaleric acid	2.5E-03	2.3E-05	7.6E-04	6.0E-04	0.3	0.040
Gly-Gly	2.2E-03	2.4E-04	6.3E-04	N.A.	0.3	N.A.
Pyridoxine	2.1E-03	1.9E-04	5.9E-04	4.2E-04	0.3	0.091
Carnitine	7.7E-02	1.6E-03	2.1E-02	1.3E-02	0.3	0.015
Gly-Asp	4.5E-03	3.3E-04	1.2E-03	6.9E-04	0.3	0.006
Diethanolamine	5.1E-03	1.6E-03	1.2E-03	1.8E-04	0.2	0.053
Pantothenic acid	3.2E-02	2.3E-03	7.1E-03	6.8E-03	0.2	0.017
Cyclohexylamine	7.2E-03	1.7E-03	1.5E-03	3.4E-04	0.2	0.026
GABA	1.2E-02	9.4E-04	2.7E-03	1.8E-03	0.2	0.004
Phosphocreatine	3.0E-02	4.9E-04	5.5E-03	5.0E-03	0.2	0.014
O-Acetylcarnitine	3.3E-02	1.0E-03	6.0E-03	6.1E-03	0.2	0.015
Fructose 1,6-diphosphate	1.5E-02	1.5E-03	2.4E-03	1.6E-03	0.2	0.009
PRPP	4.4E-03	1.5E-03	6.8E-04	N.A.	0.2	N.A.
β-Ala	1.7E-01	1.2E-02	1.0E-02	1.1E-02	0.1	6.0E-05

^aS.D., standard deviation; N.D., not detected; N.A., not available.

^bp values are calculated by Welch's t-test between fetal and adult hepatocytes.

formed on both the metabolite and sample axes. The dendrogram of HCA showed that the adult hepatocytes were well-distinguished from the fetal hepatocytes (Supplementary Fig. S2).

Next, the relative amounts of metabolites were compared between fetal and adult hepatocytes and those that displayed greater than 5-fold or less than 0.3-fold

change in adult hepatocytes were listed (Table 1). Highly increased metabolites in the adult hepatocytes included glycolysis/glyconeogenesis intermediates, some amino acids, and TCA and urea cycle intermediates; decreased metabolites were glycolysis/glyconeogenesis intermediates and metabolites involved in β-oxidation of fatty acids. This trend was consistent with the PCA results described

Metabolome analysis of human fetal and adult hepatocytes

above. Statistically significant differences in the relative amounts of metabolites between fetal and adult hepatocytes were not found in metabolites that were increased in the adult hepatocytes, because of the variation between adult hepatocyte samples.

Energy metabolism

We first compared the relative amounts of glycolysis/glyconeogenesis and TCA cycle metabolites between human fetal and adult hepatocytes (Fig. 2), because it was previously reported that fetal hepatocytes are glycolytic and have few mitochondria, suggesting their energy production is lower than that of adult hepatocytes in rat (Burch *et al.*, 1963; Oliver *et al.*, 1983; Vergonet *et al.*, 1970). Our results showed that the levels of glucose 6-phosphate (3.5-fold), fructose 6-phosphate (2.3-fold) and phosphoenolpyruvic acid (2.1-fold) in glycolysis/glyconeogenesis, and fumaric acid (5.8-fold), 2-oxoglutaric acid (4.8-fold), malic acid (4.2-fold) and succinic acid (3.5-fold) in the TCA cycle were higher in the adult compared with the fetal hepatocytes. In contrast, fructose 1,6-diphosphate in glycolysis/glyconeogenesis was significantly lower (0.2-fold, $p = 0.009$) (Fig. 2, Table 1 and Supplementary Table S2). In addition, among the metabolites involved in β -oxidation of fatty acids, the level of glycerol 3-phosphate which is required for synthesis of diacylglycerol and triacylglycerol, was 17.7-fold higher in the adult compared with the fetal hepatocytes, whereas levels of carnitine and *O*-acetylcarnitine which are required for transport of fatty acids into mitochondria from the cytoplasm, were lower (0.3-fold, $p = 0.015$ for carnitine, and 0.2-fold, $p = 0.015$ for *O*-acetylcarnitine, respectively) (Table 1). These results are consistent with previous findings that fetal hepatocytes are glycolytic and possess low mitochondrial activity, and suggest that the pathways of glyconeogenesis and β -oxidation of fatty acid are activated in adult hepatocytes. In fact, the fetus depends on the umbilical supply of glucose via the placenta. Under physiological condition, glucose is not only oxidized to CO_2 but also used to synthesis of new structural components and energy storage materials such as glycogen and fat (Fowden, 1994).

Urea cycle

The relative amounts of urea cycle metabolites were compared between fetal and adult hepatocytes (Fig. 3). The relative amounts of ornithine (59.8-fold), urea (11.1-fold) and citrulline (6.1-fold) were higher in adult compared to fetal hepatocytes (Table 1). The expression levels of urea cycle enzymes were measured by real-time PCR assays and compared between fetal and adult

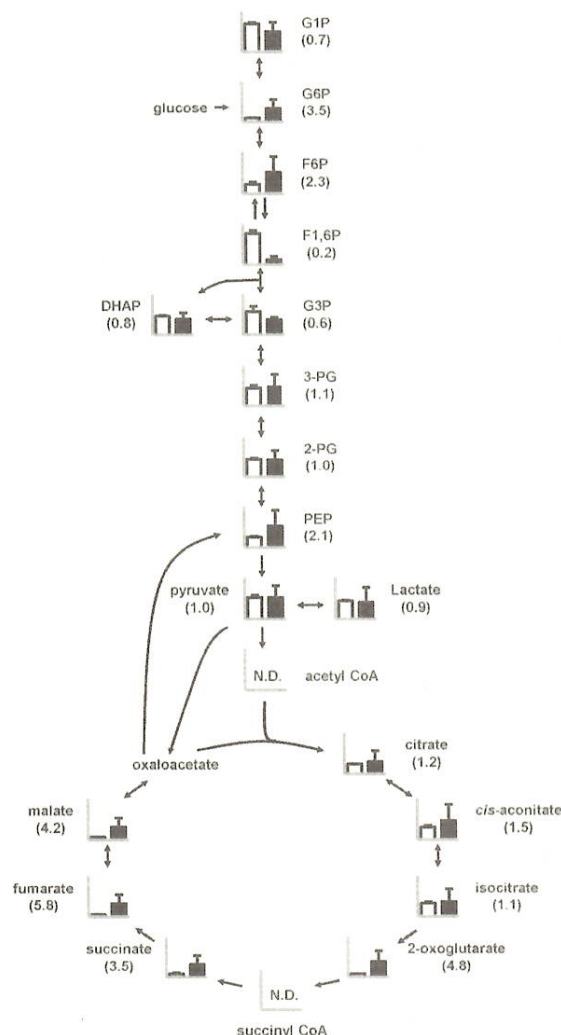


Fig. 2. Comparison of relative amounts of glycolysis and TCA cycle-related metabolites in human fetal (open box) and adult (closed box) hepatocytes using CE-TOFMS. N.D. indicates "not detected". The columns represent relative average amounts and error bars indicate SD. Numbers below the metabolite name represent the ratio of relative amounts of metabolites from the adult hepatocytes to those from the fetal hepatocytes. The abbreviations are as follows: G1P, glucose 1-phosphate; G6P, glucose 6-phosphate; F6P, fructose 6-phosphate; F1,6P, fructose 1,6-diphosphate; DHAP, dihydroxyacetone phosphate; G3P, glyceraldehyde 3-phosphate; 3-PG, 3-phosphoglycerate; 2-PG, 2-phosphoglycerate; PEP, phosphoenolpyruvate.

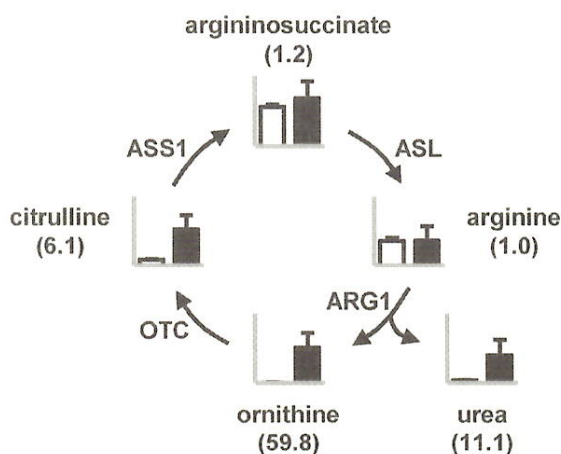


Fig. 3. Comparison of relative amounts of urea cycle metabolites in human fetal (open box) and adult (closed box) hepatocytes using CE-TOFMS. The columns represent relative average amounts and error bars indicate SD. Numbers below the metabolite name represent the ratio of relative amounts of metabolites from the adult hepatocytes to those from the fetal hepatocytes. The abbreviations are as follows: ASS1, argininosuccinate synthase 1; ASL, argininosuccinate lyase; ARG1, arginase; OTC, ornithine transcarbamylase.

hepatocytes (Fig. 4). The results showed that the expression levels of ASS1 and ASL were significantly higher in the adult compared to the fetal hepatocytes (2.6-fold, $p = 0.014$ for ASS1, and 10.4-fold, $p = 0.027$ for ASL, respectively). Moreover, expression of ARG1 and OTC was detected only in the adult, and not in the fetal hepatocytes. These results indicated that the adult hepatocytes could metabolize the ammonium produced during amino acid metabolism through the urea cycle, whereas the fetal hepatocytes could not.

The lower levels of the urea cycle and TCA cycle metabolites in the fetal hepatocytes are closely related to mitochondrial function. The numbers of mitochondria in mouse hepatocytes were low in the prenatal stage and increased through development and aging of animals (Nagata, 2006). This indicates that energy metabolism differs in fetal and adult hepatocytes and is consistent with previous findings that fetal hepatocytes are glycolytic (Vergonet *et al.*, 1970).

The liver is the first site of contact with xenobiotics, it possesses a high metabolic capacity and has been frequently investigated as a target of toxicity. In adults, the mechanisms of hepatotoxicity are well understood for

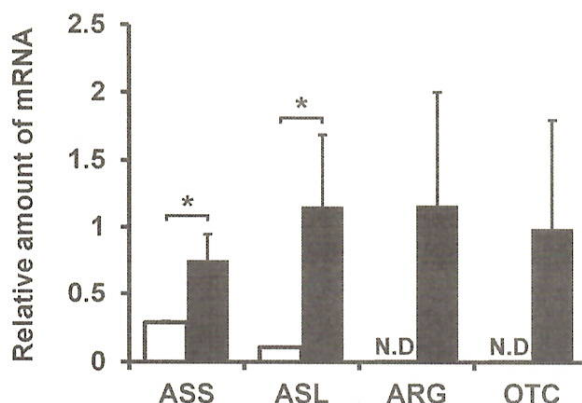


Fig. 4. Quantification of mRNA of urea cycle enzymes by TaqMan real-time RT-PCR in human fetal (open box) and adult (closed box) hepatocytes. mRNA expression levels of urea cycle enzymes were normalized with β -actin mRNA levels. The results indicate the mean \pm S.D. *, $p < 0.05$ and N.D., not detected. The abbreviations are as in Fig. 3.

many hepatotoxicants. However, it is known that the sensitivity of fetal hepatocytes to chemical compounds is distinct from that of adult hepatocytes (Shankar and Mehendale, 2010). Most drugs and xenobiotics have molecular weight less than 500 Da and easily cross the placenta to enter the fetal compartment (Evans and Ganjam, 2011). Although systems for evaluating the toxicity of several drug and chemical compounds have been studied for adult liver, such systems have not been elucidated for prenatal or neonatal human liver. Progressive changes in the production of liver-specific enzymes and proteins during normal development generally occur at three specific developmental stages: (1) late gestation, (2) at or directly following birth, and (3) just prior to weaning (Greengard, 1977). We are now proceeding with experiments to construct evaluation systems for toxicity of drugs and chemical compounds in the prenatal period, based on the differences of basal metabolic functions between fetal and adult hepatocytes.

In conclusion, comprehensive metabolome analysis of human fetal and adult hepatocytes was performed by CE-TOFMS and 211 ionic metabolites (116 anion and 95 cation) were identified. Comparison of the relative amounts of metabolites between fetal and adult hepatocytes showed that some metabolites in glycolysis/glyconeogenesis, the TCA cycle and the urea cycle were lower in fetal hepatocytes than in adult hepatocytes. These results provide useful, fundamental information for stud-

Metabolome analysis of human fetal and adult hepatocytes

ies on the basal metabolic functions of human fetal and adult hepatocytes.

ACKNOWLEDGMENT

This work was supported by a Health and Labor Science Research Grant from the Ministry of Health, Labor and Welfare in Japan.

Conflict of interest--- The authors declare that there is no conflict of interest.

REFERENCES

- Arias, I., Wolkoff, A., Boyer, J., Shafritz, D., Fausto, N., Alter, H. and Cohen, D. (2009): *The Liver: Biology and Pathobiology*, 5th edition. Wiley-Blackwell, New Jersey.
- Burch, H.B., Lowry, O.H., Kuhlman, A.M., Skerjance, J., Diamant, E.J., Lowry, S.R. and Von Dippe, P. (1963): Changes in patterns of enzymes of carbohydrate metabolism in the developing rat liver. *J. Biol. Chem.*, **238**, 2267-2273.
- Chinnici, C.M., Timoneri, F., Amico, G., Pietrosi, G., Vizzini, G., Spada, M., Pagano, D., Gridelli, B. and Conaldi, P.G. (2014): Characterization of liver-specific functions of human fetal hepatocytes in culture. *Cell Transplant.*, DOI:10.3727/096368914X680082.
- Delneri, D., Brancia, F.L. and Oliver, S.G. (2001): Towards a truly integrative biology through the functional genomics of yeast. *Curr. Opin. Biotechnol.*, **12**, 87-91.
- Dumas, M.E., Kinross, J. and Nicholson, J.K. (2014): Metabolic phenotyping and systems biology approaches to understanding metabolic syndrome and fatty liver disease. *Gastroenterology*, **146**, 46-62.
- Evans, T.J. and Ganjam, V.K. (2011): Reproductive anatomy and physiology. In *Reproductive and Developmental Toxicology*. (Gupta R.C., ed.), pp.7-32, Academic Press/ Elsevier, Inc., New York.
- Fowden, A.L. (1994): Fetal metabolism and energy balance. In *Textbook of Fetal Physiology*. (Thorburn, G.D. and Harding, R., ed.), pp.70-82, Oxford Medical Publications, Oxford.
- Greengard, O. (1977): Enzymic differentiation of human liver: comparison with the rat model. *Pediatr. Res.*, **11**, 669-676.
- Hirayama, A., Kami, K., Sugimoto, M., Sugawara, M., Toki, N., Onozuka, H., Kinoshita, T., Saito, N., Ochiai, A., Tomita, M., Esumi, H. and Soga, T. (2009): Quantitative metabolome profiling of colon and stomach cancer microenvironment by capillary electrophoresis time-of-flight mass spectrometry. *Cancer Res.*, **69**, 4918-4925.
- Houtkooper, R.H., Argmann, C., Houten, S.M., Cantó, C., Jenning, E.H., Andreux, P.A., Thomas, C., Doenlen, R., Schoonjans, K. and Auwerx, J. (2011): The metabolic footprint of aging in mice. *Sci. Rep.*, 134.10.1038/srep00134.
- Jang, Z.H., Chung, H.C., Ahn, Y.G., Kwon, Y.K., Kim, J.S., Ryu, J.H., Ryu, D.H., Kim, C.H. and Hwang, G.S. (2012): Metabolic profiling of an alcoholic fatty liver in zebrafish (*Danio rerio*). *Mol. Biosyst.*, **8**, 2001-2009.
- Junker, B.H., Klukas, C. and Schreiber, F. (2006): VANTED: A system for advanced data analysis and visualization in the context of biological networks. *BMC Bioinformatics*, **7**, 109.
- Kami, K., Fujimori, T., Sato, H., Sato, M., Yamamoto, H., Ohashi, Y., Sugiyama, N., Ishihama, Y., Onozuka, H., Ochiai, A., Esumi, H., Soga, T. and Tomita, M. (2013): Metabolomic profiling of lung and prostate tumor tissues by capillary electrophoresis time-of-flight mass spectrometry. *Metabolomics*, **9**, 444-453.
- Matsushita, T., Nakano, K., Nishikura, Y., Higuchi, K., Kiyota, A. and Ueoka, R. (2003): Spheroid formation and functional restoration of human fetal hepatocytes on poly-L-amino acid-coated dishes after serial proliferation. *Cytotechnology*, **42**, 57-66.
- Monton, M.R. and Soga, T. (2007): Metabolome analysis by capillary electrophoresis-mass spectrometry. *J. Chromatogr. A*, **1168**, 237-246.
- Nagata, T. (2006): Electron microscopic radioautographic study on protein synthesis in hepatocyte mitochondria of aging mice. *ScientificWorldJournal*, **6**, 1583-1598.
- Oliver, I.T., Martin, R.L., Fisher, C.J. and Yeoh, G.C. (1983): Enzymic differentiation in cultured foetal hepatocytes of the rat. Induction of serine dehydratase activity by dexamethasone and dibutyryl cyclic AMP. *Differentiation*, **24**, 234-238.
- Panduro, A., Shalaby, F. and Shafritz, D.A. (1987): Changing patterns of transcriptional and post-transcriptional control of liver-specific gene expression during rat development. *Genes Dev.*, **1**, 1172-1182.
- Preidis, G.A., Keaton, M.A., Campeau, P.M., Bessard, B.C., Conner, M.E. and Hotez, P.J. (2014): The undernourished neonatal mouse metabolome reveals evidence of liver and biliary dysfunction, inflammation, and oxidative stress. *J. Nutr.*, **144**, 273-281.
- Shankar, K. and Mehendale, H.M. (2010): Developmental toxicology of the liver. In *Reproductive Toxicology*, third edition. (Kapp, Jr., R.W. and Tyl, R.W., ed.), pp.205-222, Informa Healthcare, London.
- Sharma, N., Schloss, R. and Yarmush, M. (2008): What came first: fully functional or metabolically mature liver? *Crit. Rev. Biomed. Eng.*, **36**, 413-439.
- Shimada, T., Yamazaki, H., Mimura, M., Wakamiya, N., Ueng, Y.F., Guengerich, F.P. and Inui, Y. (1996): Characterization of microsomal cytochrome P450 enzymes involved in the oxidation of xenobiotic chemicals in human fetal liver and adult lungs. *Drug Metab. Dispos.*, **24**, 515-522.
- Soga, T., Ishikawa, T., Igarashi, S., Sugawara, K., Kakazu, Y. and Tomita, M. (2007): Analysis of nucleotides by pressure-assisted capillary electrophoresis-mass spectrometry using silanol mask technique. *J. Chromatogr. A*, **1159**, 125-133.
- Sugimoto, M., Wong, D.T., Hirayama, A., Soga, T. and Tomita, M. (2010): Capillary electrophoresis mass spectrometry-based saliva metabolomics identified oral, breast and pancreatic cancer-specific profiles. *Metabolomics*, **6**, 78-95.
- Uehara, T., Ono, A., Maruyama, T., Kato, I., Yamada, H., Ohno, Y. and Urushidani, T. (2010): The Japanese toxicogenomics project: application of toxicogenomics. *Mol. Nutr. Food Res.*, **54**, 218-227.
- Vergonet, G., Hommes, F.A. and Molenaar, I. (1970): A morphometric and biochemical study of fetal and adult rat liver cells, with special reference to energy metabolism. *Biol. Neonate*, **16**, 297-305.
- Xie, Z., Li, H., Wang, K., Lin, J., Wang, Q., Zhao, G., Jia, W. and Zhang, Q. (2010): Analysis of transcriptome and metabolome profiles alterations in fatty liver induced by high-fat diet in rat. *Metabolism*, **59**, 554-560.
- Zaret, K.S. (2008). Genetic programming of liver and pancreas progenitors: lessons for stem-cell differentiation. *Nat. Rev. Genet.*, **9**, 329-340.
- Zhao, R. and Duncan, S.A. (2005). Embryonic development of the liver. *Hepatology*, **41**, 956-967.

SHORT COMMUNICATION

Simple *in vitro* migration assay for neural crest cells and the opposite effects of all-*trans*-retinoic acid on cephalic- and trunk-derived cells

Makoto Usami¹, Katsuyoshi Mitsunaga², Tomohiko Irie¹, Atsuko Miyajima³, and Osamu Doi⁴

Divisions of ¹Pharmacology and ²Medical Devices, National Institute of Health Sciences, Tokyo, ³School of Pharmaceutical Sciences, Toho University, Chiba, and ⁴Laboratory of Animal Reproduction, United Graduate School of Agricultural Science, Gifu University, Gifu, Japan

ABSTRACT Here, we describe a simple *in vitro* neural crest cell (NCC) migration assay and the effects of all-*trans*-retinoic acid (RA) on NCCs. Neural tubes excised from the rhombencephalic or trunk region of day 10.5 rat embryos were cultured for 48 h to allow emigration and migration of NCCs. Migration of NCCs was measured as the change in the radius (radius ratio) calculated from the circular spread of NCCs between 24 and 48 h of culture. RA was added to the culture medium after 24 h at embryotoxic concentrations determined by rat whole embryo culture. RA (10 μM) reduced the migration of cephalic NCCs, whereas it enhanced the migration of trunk NCCs, indicating that RA has opposite effects on these two types of NCCs.

Key Words: developmental toxicity, embryo, migration assay, neural crest cell, rat

INTRODUCTION

In vertebrate development, neural crest cells (NCCs) migrate from the neural primordia throughout the embryo and contribute to morphogenesis (Douarin and Kalcheim 1999). Malfunction of NCCs leads to dysmorphologies, tumors, and syndromes called neurocristopathies (Hall 2009). In developmental toxicology, it has been proposed that altered migration of cephalic NCCs induced by chemicals leads to fetal malformation. For example, retinoic acids and fluconazole inhibited the migration of cephalic NCCs, causing branchial abnormalities in cultured rat and mouse embryos (Pratt et al. 1987; Menegola et al. 2004). These abnormalities are considered to result in *in vivo* craniofacial malformations, such as the cleft palate, cleft lip, micrognathia, and thymic agenesis (Hall 2009).

However, the effects of developmental toxicants on the migration of NCCs in mammals have not been fully investigated because no convenient experimental methods are available. Migration of NCCs is usually examined by time-lapse video imaging of *in vitro* cultured cells (Fuller et al. 2002) or *in vivo* fluorescently labeled cells (Kawakami et al. 2011). These methods are time-consuming and are not suitable for developmental toxicity investigations of chemicals.

In the present study, we have described a simple migration assay that enables investigation of the effects of chemicals on rat NCCs. Cephalic or trunk NCCs were cultured as emigrants from isolated neural tubes of day 10.5 rat embryos. The cultured NCCs were

exposed to test chemicals for 24 to 48 h, and their migration was determined as the change in the radius calculated from the circular spread of the NCCs during exposure. By using this assay method, we found that RA has opposite effects on the migration of cephalic and trunk NCCs.

MATERIALS AND METHODS

Animals

Wistar rats (Crj:WI; Charles River Japan, Kanagawa, Japan) were used in these assays. Pregnant rats were obtained by mating female and male rats overnight, and the plug day was designated as day 0.5 of gestation. All the animal experiments were performed in accordance with the guidelines for animal experiments of the National Institute of Health Sciences.

Rat whole embryo culture

Rat embryos on day 10.5 of gestation were cultured for 24 h by the roller bottle method as described previously (Usami et al. 2008). All-*trans*-retinoic acid (RA, CAS 302-79-4; Wako Pure Chemical Industries, Osaka, Japan) was dissolved in dimethyl sulfoxide before adding it to the culture medium, which was rat serum. Control embryos were cultured in the presence of the same concentration of dimethyl sulfoxide.

NCC culture

Neural crest cells were cultured as emigrated cells from the neural tubes of day 10.5 rat embryos, as outlined in Figure 1A. Neural tubes were excised from the rhombencephalic or trunk region of the embryos in Hanks' balanced salt solution with sharpened tungsten needles. The excised neural tubes (approximately 0.7 mm long) were cut open dorsally and attached to the 35-mm culture dishes (BD Primaria; Becton Dickinson, Franklin Lakes, NJ, USA) containing 2 mL of Dulbecco's Modified Eagle Medium with high glucose (DMEM; Gibco, Life Technologies, Carlsbad, CA, USA) and 10% (v/v) fetal bovine serum (Gibco) (Fig. 1B,C). The dishes were incubated at 37°C with 5% CO₂ for 48 h. After 24 h of culture, the medium was replaced with medium containing RA dissolved in dimethyl sulfoxide (final concentration, 0.1% v/v).

Observation and analysis of cultured NCCs

Neural crest cells emigrated from the neural tubes were observed for their attachment to the surface of the culture vessels and the extent of migration. Images of cultured NCCs were recorded digitally with a phase-contrast microscope (BZ-9000; Keyence, Osaka, Japan) after 24 and 48 h of culture. NCCs that did not completely surround the neural tube after 24 h of culture and those cultures in

Correspondence: Makoto Usami, PhD, Division of Pharmacology, National Institute of Health Sciences, 1-18-1, Kamiyoga, Setagaya, Tokyo 158-8501, Japan. Email: usami@nihs.go.jp

Received January 8, 2014; revised and accepted March 31, 2014.

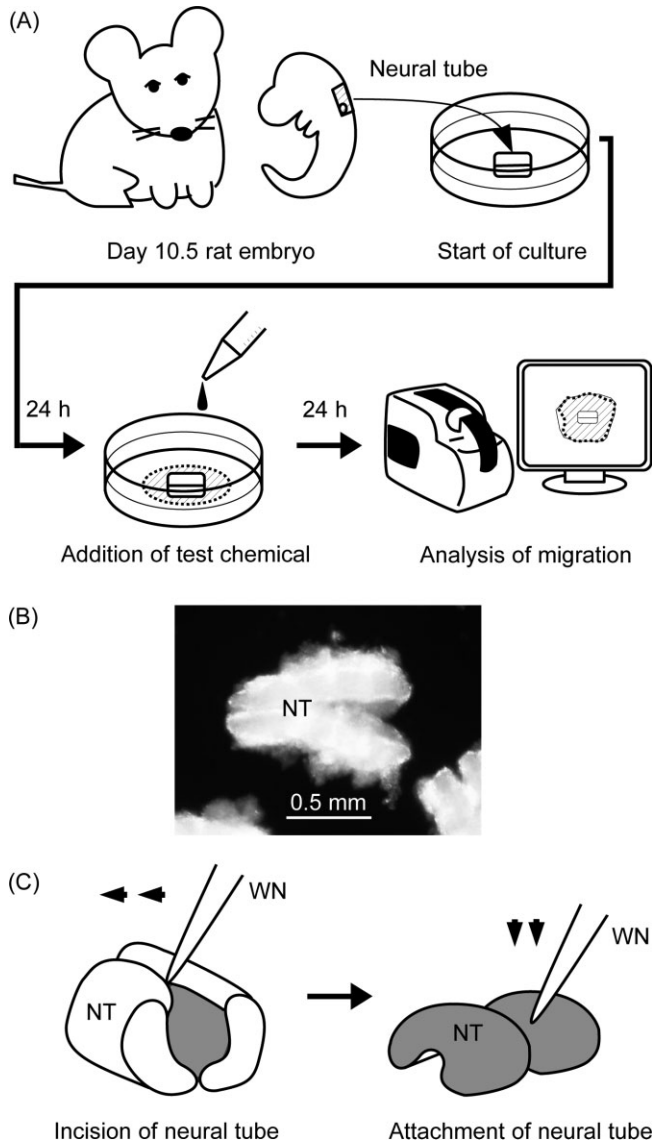


Fig. 1 Outline of the neural crest cell (NCC) migration assay. (A) Neural tubes were excised from the rhombencephalic region of day 10.5 rat embryos and cultured for 48 h to allow emigration of the NCCs. Test chemicals were added to the culture medium after 24 h of culture. Migration indices were calculated as the circular spread of NCCs after 24 and 48 h of culture. (B) A dorsal view of a neural tube prepared for culture. The right side is cranial. (C) Neural tubes were incised dorsally and pressed to the culture plate surface with the outer wall downward using a tungsten needle. It should be noted that the neural tubes became concave outward after the incision. NT, neural tube. WN, tungsten needle.

which the neural tube detached from the surface of the culture vessel before the end of the culture period were omitted from the analyses because they showed little migration.

The migration distance of the NCCs was calculated as the increase in the radius of the circular spread between 24 and 48 h of culture. The digital images of cultured NCCs were analyzed by using ImageJ software (<http://rsb.info.nih.gov/ij/>, 1997–2009; Rasband, W.S., ImageJ, U. S. National Institutes of Health, Bethesda, MD, USA). The outermost NCCs in each of the cultured neural tubes were connected with the polygon tool as if a rubber

band were placed around the cells, and the pixel count inside the polygon was measured. Considering the polygon as a circle, its radius was calculated as follows:

$$\text{Radius} = \sqrt{(\text{number of pixels in polygon} / \pi)}$$

To assess NCC migration, the radius ratio was calculated using the following formula:

$$\text{Radius ratio} = (\text{radius at 48 h} - \text{radius at 24 h}) / \text{radius at 24 h}$$

This ratio was then normalized to the control to allow for comparisons between experiments.

Immunocytochemistry

At the end of the culture period, the neural tubes and non-NCCs derived from surrounding tissues were removed with tungsten needles under a stereomicroscope, leaving the emigrated cells in the dish. The emigrated cells were fixed with 4% (w/v) paraformaldehyde in phosphate-buffered saline (PBS) for 20 min, permeated with 0.1% Triton X-100 in PBS for 2 min, and blocked with 3% (w/v) bovine serum albumin (BSA) in PBS for 30 min at room temperature. The treated cells were incubated with a primary antibody in 1% (w/v) BSA-PBS for 1 h, and then incubated with a secondary antibody in 1% (w/v) BSA-PBS for 1 h at room temperature. The primary antibodies used were an anti-HNK-1 mouse IgM monoclonal antibody (CBL519; Merck KGaA, Darmstadt, Germany) and an anti-SOX10 mouse IgG monoclonal antibody (MAB2864; R & D Systems, Minneapolis, MN), and the secondary antibodies used were fluorescently labeled anti-mouse (Alexa Fluor 488 goat anti-mouse IgM, A-21042; Invitrogen, Life Technologies) and anti-rabbit (Alexa Fluor 594 goat anti-mouse IgG (H + L), A-11005; Invitrogen) antibodies. To stain the cell nuclei, 4',6-diamidino-2-phenylindole (DAPI, D-1306; Invitrogen) dissolved in methanol (2 mg/mL) was added to the secondary antibody solutions at a concentration of 0.1% (v/v). The immunostained cells were photographed with a fluorescence microscope (BZ-9000, equipped with the DAPI-BP, GFP-BP, and Texas Red filters; Keyence).

Statistical analysis

Statistical significance of the difference between the experimental groups was examined by the Student's *t*-test or Fisher's exact test.

RESULTS

Identification of NCCs

Cells emigrated from explanted rhombencephalic and trunk neural tubes during culture were identified as NCCs by immunocytochemistry of the following marker antigens, HNK-1 (Nagase et al. 2003) on the cell membrane and SOX10 (Kim et al. 2003) in the cell nucleus. The nuclei of the emigrated cells were stained by DAPI and the anti-SOX10 antibody, and the cells were stained by the anti-HNK-1 antibody (Fig. 2A–C). The merged images showed the co-expression of HNK-1 and SOX10 in the emigrated cells at least in the periphery of the circular spread (Fig. 2D). Thus, the emigrated cells were identified as NCCs.

Analysis of NCC migration

Figure 3A shows images of NCCs after 24 and 48 h of culture. The migration of NCCs was calculated as the difference in the radius of the circular spread of the cells between 24 and 48 h of culture because it was impossible to determine the migration distance from

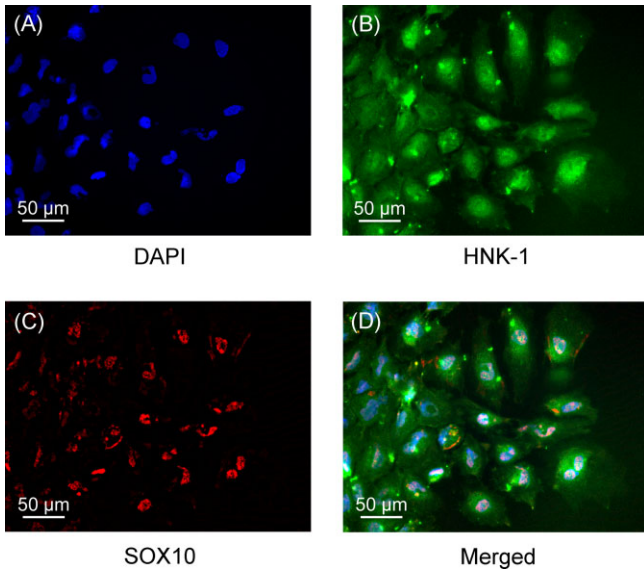


Fig. 2 Immunocytochemical identification of neural crest cells (NCCs). (A) Nuclear staining with 4'6'-diamidino-2-phenylindole dihydrochloride (DAPI). (B) Staining of the cell membrane with an anti-HNK-1 antibody. (C) Staining of nuclei with an anti-SOX10 antibody. (D) A merged image of A, B, and C.

the neural tube since its outline was obscured during culture, and individual NCCs could not be distinguished. The mean migration distance of the NCCs calculated using this method was approximately 500 µm during the 24-h culture period. To evaluate NCC migration, the radius ratio was used because this ratio showed less variability than the radius difference as determined by the coefficient of variation, suggesting the dependence of NCC migration on the size of the explanted neural tubes (Fig. 3B).

Effects of RA on cultured rat embryos

Embryotoxic concentrations of RA were determined by rat whole embryo culture to compare RA-induced embryotoxicity to the effects of RA on NCC migration. RA was toxic to cultured rat embryos at concentrations ≥ 3 µM, which caused a reduction in the number of somite pairs and an increased incidence of morphological abnormalities (Table 1). Deformed branchial arches, more specifically, the hypoplastic 3rd branchial arch, were observed at 10 µM RA but not at 3 µM (Fig. 4). These embryotoxic concentrations were comparable to those in the maternal plasma (about 4.5 µg/mL = 15 µM) obtained by the administration of a teratogenic dose (10 mg/kg) of RA to mice (Kraft 1992), and the observed abnormalities corresponded to *in vivo* malformations of the ear, eye, and thymus. Based on these results, RA was added at 0, 3, and 10 µM during the 24-h exposure period in the following NCC migration experiments.

Effects of RA on NCC migration

Rat NCCs emigrated from the neural tube were exposed to embryotoxic concentrations of RA for 24 h. RA reduced the migration of cephalic NCCs in a concentration dependent manner, and 10 µM RA reduced the migration by approximately 10% (Fig. 5A). In contrast, RA (10 µM) enhanced the migration of trunk NCCs by

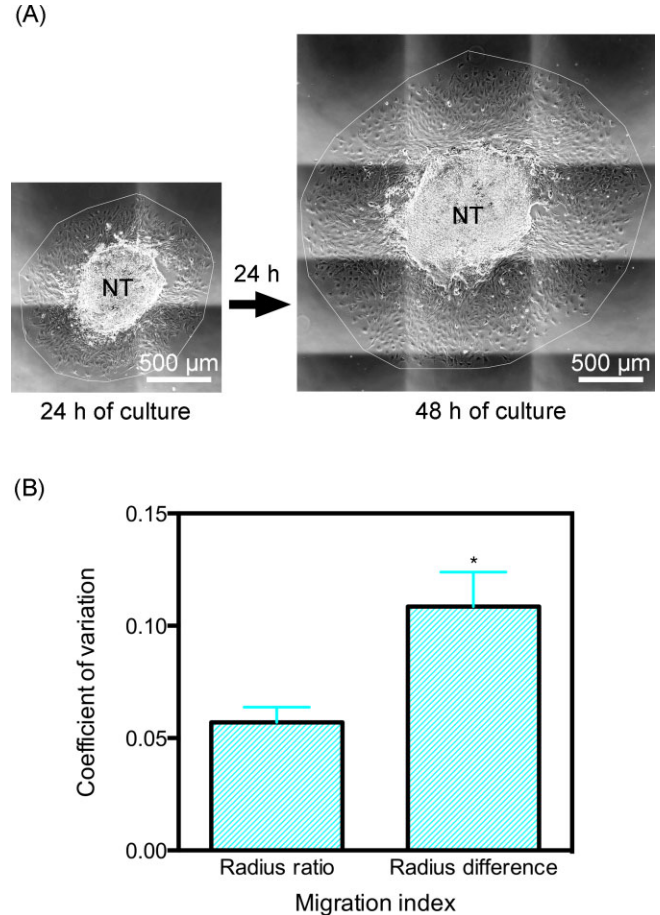


Fig. 3 Analysis of neural crest cell (NCC) migration. (A) Cultured NCCs were enclosed in a polygon to calculate the migration indices after 24 and 48 h of culture. (B) Comparison of migration indices. The means \pm standard error of the mean (SEM) of the coefficient of variation from eight control cultures are shown for the migration indices: the radius ratio and the radius difference.

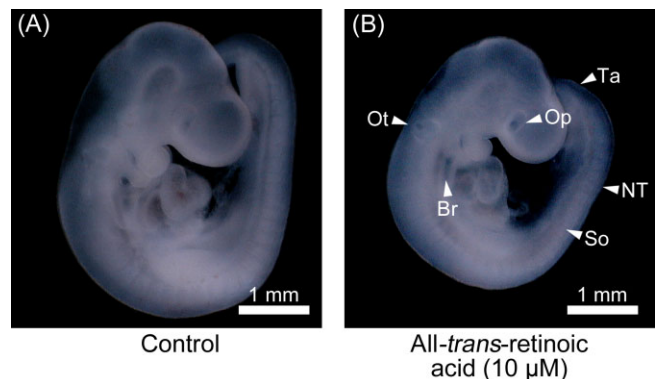


Fig. 4 Appearance of rat embryos cultured in the presence of all-*trans*-retinoic acid. Rat embryos after 24 h of culture are shown after removal of the embryonic membranes. Arrowheads indicate deformed organs. Br, branchial arch; NT, neural tube; Op, optic vesicle; Ot, otic vesicle; So, somite; Ta, tail.

Table 1 Growth of day 10.5 rat embryos cultured in the presence of all-*trans*-retinoic acid (RA)

	All- <i>trans</i> -retinoic acid (μM)			
	0 (Control)	1	3	10
No. embryos	6	6	6	6
No. viable embryos	6 (100%)	6 (100%)	6 (100%)	5 (83.3%)
Crown-rump length (mm)	4.28 \pm 0.05	4.45 \pm 0.07	4.29 \pm 0.05	4.12 \pm 0.22
Head length (mm)	2.34 \pm 0.04	2.40 \pm 0.04	2.34 \pm 0.06	2.19 \pm 0.13
No. somite pairs	27.7 \pm 0.21	27.5 \pm 0.22	27.0 \pm 0.37	25.6 \pm 0.60**
No. embryos with deformed organ	0	0	5 (83.3%)**	5 (100%)**
Branchial arch	0	0	0	4 (80.0%)*
Neural tube	0	0	5 (83.3%)**	5 (100%)**
Optic vesicle	0	0	5 (83.3%)**	4 (80.0%)*
Otic vesicle	0	0	5 (83.3%)**	5 (100%)**
Somite	0	0	2 (33.3%)	3 (60.0%)
Tail	0	0	2 (33.3%)	1 (20.0%)

Embryos were cultured for 24 h by the roller method in the medium composed of pure rat serum. Mean \pm standard error of the mean (SEM) is shown. Asterisks indicate significant difference from the control value (* $P < 0.05$; ** $P < 0.01$).

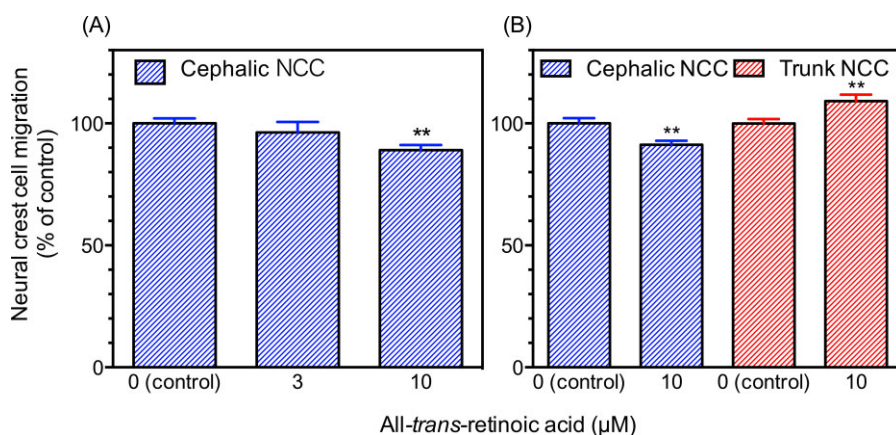


Fig. 5 Neural crest cell (NCC) migration during 24 h of culture in the presence of all-*trans*-retinoic acid (RA). (A) Effects of RA on cephalic NCCs. (B) Effects of RA on trunk NCCs. NCC migration was calculated as the ratio of the radius from the circular spread of the NCCs and was normalized to the control. The means \pm standard error of the mean (SEM) of 9–11 neural tubes are shown. Asterisks indicate statistically significant differences from the corresponding control (** $P < 0.01$).

approximately 10%, indicating the RA has opposite effects on cephalic and trunk NCCs (Fig. 5B).

DISCUSSION

In the present study, we established a simple *in vitro* NCC migration assay that enabled easy assessment of the effects of chemicals on NCC migration in developmental toxicity studies. However, the present method is not suitable for screening because the concentrations found to be effective do not provide information on overall embryotoxicity. Whole embryo culture or general cytotoxicity assays in combination with the present NCC migration assay should be useful for examining the specific effects of chemicals on NCCs. One advantage of the present NCC migration assay is that general cellular techniques and toxicogenomic analyses for toxicological mechanistic studies are easily applicable to NCCs isolated by the removal of neural tubes, as described for the immunocytochemistry methodology.

By using this method, we found that RA had opposite effects on the migration of cephalic and trunk NCCs. The reduction in

cephalic NCC migration induced by RA is consistent with previous reports that described the inhibitory effects of RA on cephalic NCCs as a pathogenic mechanism underlying craniofacial malformation (Pratt et al. 1987; Menegola et al. 2004). In the present study, we observed hypoplasia of the 3rd branchial arch, the formation of which is dependent on migrated cephalic NCCs, at the same RA concentration that reduced cephalic NCC migration. Enhancement of trunk NCC migration is not directly related to any known developmental toxicity of RA. However, these opposite effects on cephalic and trunk NCCs will make it easy to investigate the mechanisms underlying RA effects on NCCs by allowing comparative analysis.

When evaluating the results of the present NCC migration assay, it should be noted that altered migration is not necessarily a direct effect of the chemical on the motility of NCCs. Because NCC migration in the present assay was determined as the circular spread of the cells, the number of cells can influence the result, that is, a decrease in the number of cells induced by cytotoxicity can result in a reduced migration index. It is also possible that altered NCC migration is due to the effects of chemicals on the neural tube. This

is because NCC migration in the present assay is dependent on the presence of a neural tube, as evidenced by the reduced migration of NCCs whose neural tube detached from the culture surface.

In conclusion, we established a simple migration assay that enables investigation of the effects of chemicals on rat NCCs. By using this assay method, we found that RA has opposite effects on the migration of cephalic and trunk NCCs.

ACKNOWLEDGMENTS

This work was supported by a Health and Labor Science Research Grant from the Ministry of Health, Labor, and Welfare of Japan.

CONFLICT OF INTEREST

The authors declare that there are no conflicts of interest.

REFERENCES

- Douarin NL, Kalcheim C. 1999. The neural crest, 2nd edn, Vol. 9. New York: Cambridge University Press.
- Fuller LC, Cornelius SK, Murphy CW, Wiens DJ. 2002. Neural crest cell motility in valproic acid. *Reprod Toxicol* 16:825–839.
- Hall BK. 2009. Neurocristopathies. In: The neural crest and neural crest cells in vertebrate development and evolution, 2nd edn. New York: Springer. p 269–293.
- Kawakami M, Umeda M, Nakagata N, Takeo T, Yamamura K-I. 2011. Novel migrating mouse neural crest cell assay system utilizing P0-Cre/EGFP fluorescent time-lapse imaging. *BMC Dev Biol* 11:68.
- Kim J, Lo L, Dormand E, Anderson DJ. 2003. SOX10 maintains multipotency and inhibits neuronal differentiation of neural crest stem cells. *Neuron* 38:17–31.
- Kraft J. 1992. Pharmacokinetics, placental transfer, and teratogenicity of 13-*cis*-retinoic acid, its isomer, and metabolites. In: Morriss-Kay GM, editor. Retinoids in normal development and teratogenesis. New York: Oxford University Press. p 267–280.
- Menegola E, Broccia ML, Di Renzo F, Massa V, Giavini E. 2004. Relationship between hindbrain segmentation, neural crest cell migration and branchial arch abnormalities in rat embryos exposed to fluconazole and retinoic acid *in vitro*. *Reprod Toxicol* 18:121–130.
- Nagase T, Sanai Y, Nakamura S, Asato H, Harii K, Osumi N. 2003. Roles of HNK-1 carbohydrate epitope and its synthetic glucuronyltransferase genes on migration of rat neural crest cells. *J Anat* 203:77–88.
- Pratt RM, Goulding EH, Abbott BD. 1987. Retinoic acid inhibits migration of cranial neural crest cells in the cultured mouse embryo. *J Craniofac Genet Dev Biol* 7:205–217.
- Usami M, Mitsunaga K, Nakazawa K, Doi O. 2008. Proteomic analysis of selenium embryotoxicity in cultured postimplantation rat embryos. *Birth Defects Res B Dev Reprod Toxicol* 83:80–96.

LETTER TO THE EDITOR

Various definitions of reproductive indices: A proposal for combined use of brief definitions

Several reproductive indices, such as live birth index, are calculated as endpoints to be evaluated in toxicity tests concerning reproductive effects of chemicals. These indices are useful to correct for variations resulting from infertility and multiple pregnancy, for example, the varied numbers of pups, among treatment groups and dams, respectively. In the toxicity test reports, the reproductive indices are used with their definitions, usually expressed as calculation formulae, to describe what they mean.

Despite their frequent use, however, the definitions of the reproductive indices have not been standardized; that is, they are different among laboratories, and are confusing. For example, the live birth index is “number of live newborns/number of implantation sites × 100” in some laboratories, but is “number of live newborns/number of total newborns × 100” in others, as listed in Table 1. These two definitions are quite different from each other in that the latter does not involve postimplantation loss, but the former does, though the live birth index is one of the most important reproductive indices. In most toxicity test laboratories, on the other hand, the definitions of reproductive indices cannot be changed even for standardization because they are defined as a part of laboratory computer systems.

In the database era, the confusion of reproductive indices has become more serious than ever, because data from various laboratories in the toxicity databases are frequently consulted at a time as in meta-analyses for building quantitative structure-activity relationship models. In the meta-analysis of reproductive toxicity data, reproductive indices cannot be used as toxicological endpoints to be evaluated unless their definitions, usually not found in the abstract because of their lengthiness, are clearly identified.

As a solution to this issue, we here propose combined use of brief definitions that describe the meaning of the reproductive indices with simpler words than the calculation formulae, for example, “live newborn/nidation rate” for “number of live newborns/number of implantation sites × 100.” Explanatory descriptions of the reproductive indices with their brief definitions, for example, “the live birth index (live newborn/nidation rate)” at their first appearance in the abstract and main text would be most helpful.

In this letter, we show various definitions of representative reproductive indices and propose their brief definitions. We found 14 reproductive indices with 23 definitions by a brief survey of toxicological reference books (Manson and Kang 1989; Mizutani 1992; Saikikeisei ni kansuru dejitaruka sagyogruupu iinkai 1994; Econbichon 1995; Parker 2012) and contract research organizations’ reports in a toxicological database (Japan Existing Chemical Data Base, http://dra4.nihs.go.jp/mhlw_data/jsp/SearchPage.jsp). From these indices, we show seven representative indices and 12 brief definitions as examples (Table 1), but it is not intended that the brief definitions presented here should be used as they are.

Makoto Usami¹, Katsuyoshi Mitsunaga², Tomohiko Irie¹, and Mikio Nakajima³

¹*Division of Pharmacology, National Institute of Health Sciences, Tokyo,* ²*School of Pharmaceutical Sciences, Toho University, Chiba,* and ³*Pharmaceuticals Research Center, Asahi Kasei Pharma Corporation, Shizuoka, Japan*

REFERENCES

- Econbichon DJ. 1995. Reproductive toxicology. In: Derelanko MJ, Hollinger MA, editors. *CRC handbook of toxicology*. Boca Raton: CRC Press. p 379–402.
- Manson JM, Kang YJ. 1989. Test methods for assessing female reproductive and developmental toxicology. In: Hayes AW, editor. *Principles and methods of toxicology*, 2nd edn. New York: Raven Press, Ltd. p 311–359.
- Mizutani M. 1992. Seisyoku hassei dokusei no jissai. In: Tanimura T, editor. *Developmental toxicology*. Tokyo: Chijinshokan. p 143–167. (In Japanese.)
- Parker RM. 2012. Reproductive toxicity testing-Methodology. In: Hood RD, editor. *Developmental and reproductive toxicology: a practical approach*, 3rd edn. London: Informa Healthcare. p 184–228.
- Saikikeisei ni kansuru dejitaruka sagyogruupu iinkai. 1994. Saikikeisei Yogo. In: Nakadate M, editor. *Toxicity testing*. Tokyo: National Institute of Health Sciences, Biological Safety Research Center. p 394–488. (In Japanese.) Available at URL: <http://www.nihs.go.jp/center/yougo/saiki.html>.

Correspondence: Makoto Usami, PhD, Division of Pharmacology, National Institute of Health Sciences, 1-18-1, Setagaya, Tokyo 158-8501, Japan. Email: usami@nihs.go.jp

Received August 28, 2013; revised and accepted October 29, 2013.

Table 1 Representative reproductive indices and their definitions appeared in reference books and toxicity reports

Reproductive index	Definition†									Example of brief definition
	Reference Book				Contract research organization's reproductive toxicity test report					
	Manson & Kang, 1989	Mizutani, 1992	Ecobichon, 1995	Saikikeisei, 1994	Parker, 2012	Laboratory A	Laboratory B	Laboratory C	Laboratory D	
Implantation index					Implants/Corpora lutea	Implantation sites/Corpora lutea	Implantation sites/Corpora lutea	Implantation scars/Corpora lutea	Implantation sites/Corpora lutea	Nidation/luteum rate
										Nidation/pregnant rate
Gestation index		Females with live offspring/Pregnant females		Females with live offspring/Pregnant females	Females with live born/Females with evidence of pregnancy	Females with live pups/Pregnant females				Live delivered dam/pregnant rate
Delivery index							Females which delivered live borns/Pregnant females	Dams with live offspring/Pregnant dams	Pregnant females with live pups at birth/Pregnant females	
										Newborn/nidation rate
Live birth index			(Viable pups born/litter)/(Pups born/litter)		Pups born alive/Total pups born	Live pups on lactation day 0/Pups born		Live offspring at birth/Offspring at birth	Live pups at birth/Pups born	Live/total newborn rate
										Day 1 live pup/live newborn rate
										Live newborn/nidation rate
Birth index								Live offspring at birth/Implantation scars	Live pups at birth/Implantation sites	
Viability index		Offspring alive on day 4 after birth/Live born		Offspring alive on day 4 after birth/Offspring born alive		Live pups on lactation day 4/Live pups on lactation day 0	Live pups on postnatal day 4/Live born	Live offspring at 4 days after birth/Live offsprings at birth	Live pups on postnatal day 4/Live pups at birth	Day 4 live pup/live newborn rate
										Days x/y live/live pup rate
										Live/dead newborn rate
Sex ratio (at birth)			Male offspring/Female offspring		Male offspring/Total offspring	Male pups born/Pups born		Male offspring/(Male offspring + female offspring)	Males born/Pups born	Male/total pup rate
						Live male pups/Live pups	Live born males/Live born			Live male /live total pup rate

†Common descriptions, "number of" and "× 100," are omitted.

Toxicomics Report

Proteomic analysis of ethanol-induced embryotoxicity in cultured post-implantation rat embryos

Makoto Usami¹, Katsuyoshi Mitsunaga², Tomohiko Irie¹, Atsuko Miyajima³
and Osamu Doi⁴

¹Division of Pharmacology, National Institute of Health Sciences, 1-18-1 Kamiyoga, Setagaya, Tokyo, 158-8501, Japan

²School of Pharmaceutical Sciences, Toho University, 2-2-1 Miyama, Funabashi, Chiba, 274-8510, Japan

³Division of Medical Devices, National Institute of Health Sciences, 1-18-1 Kamiyoga, Setagaya, Tokyo, 158-8501, Japan

⁴Laboratory of Animal Reproduction, United Graduate School of Agricultural Science, Gifu University, 1-1 Yanagido, Gifu, 501-1193, Japan

(Received November 9, 2013; Accepted December 18, 2013)

ABSTRACT — Protein expression changes were examined in day 10.5 rat embryos cultured for 24 hr in the presence of ethanol by using two-dimensional electrophoresis and mass spectrometry. Exposure to ethanol resulted in quantitative changes in many embryonic protein spots (16 decreased and 28 increased) at *in vitro* embryotoxic concentrations (130 and 195 mM); most changes occurred in a concentration-dependent manner. For these protein spots, 17 proteins were identified, including protein disulfide isomerase A3, alpha-fetoprotein, phosphorylated cofilin-1, and serum albumin. From the gene ontology classification and pathway mapping of the identified proteins, it was found that ethanol affected several biological processes involving oxidative stress and retinoid metabolism.

Key words: Ethanol, Embryotoxicity, Proteomics, Rat

INTRODUCTION

Developmental toxicology is a rapidly growing area of proteomics; it is expected to provide mechanistic insights and protein biomarkers for the safety evaluation of chemicals (Usami and Mitsunaga, 2011). For example, expression changes in actin-binding proteins were considered to be involved in selenate embryotoxicity in the rat whole embryo culture (Usami *et al.*, 2008). Differences in strain sensitivity to cadmium-induced teratogenicity were related to unfolded protein response process and actin polymerization in the mouse limb-bud culture (Chen *et al.*, 2008). Furthermore, based on cluster analysis of proteins with expression changes in the embryonic stem cell test, chemicals were classified into highly embryotoxic and non- or weakly embryotoxic (Groebe *et al.*, 2010). It is thus important to accumulate proteomic analysis data in the field of developmental toxicology. In the present study, protein expression changes in day 10.5 rat embryos cultured for 24 hr in the presence of ethanol, a well-known developmental toxicant, were examined by two-dimensional electrophoresis (2-DE) and mass spectrometry (MS).

MATERIAL AND METHODS

Embryo culture and ethanol treatment

Day 10.5 embryos (plug day = day 0.5) of Wistar rats (Crj: WI, Charles River Laboratories Japan, Inc., Kanagawa, Japan) were cultured for 24 hr (Usami *et al.*, 2008). Ethanol was diluted in Hank's balanced salt solution in two-fold and added to the culture medium composed of 100% rat serum at concentrations of 0, 65, 130, and 195 mM. Medium-sized cultured embryos (four embryos per treatment group) were selected for subsequent protein analyses. All animal experiments were carried out according to the guidelines for animal use of the National Institute of Health Sciences.

2-DE and MS analyses of embryonic protein

The analyses of 2-DE gels (one embryo per gel, four gels per treatment group) were carried out as previously reported (Usami *et al.*, 2009), except that the gels were stained with a fluorescent dye (Flamingo gel stain, Bio-Rad, Hercules, CA, USA) and scanned with a laser scanner (FLA-5100, GE Healthcare UK Ltd., Amersham Place, Little Chalfont, UK) at an excitation wavelength of

Correspondence: Makoto Usami (E-mail: usami@nihs.go.jp)

473 nm. Quantitative differences in protein spots of more than 1.5-fold with statistical significance by the *t*-test at 5% probability level between the control and 195 mM ethanol groups, were regarded as ethanol-induced protein expression changes.

Classification and mapping of identified proteins

NCBI nr GI numbers of the identified proteins were mapped to UniProtKB AC, and gene ontology (GO) terms were assigned using the UniProt web site (<http://www.uniprot.org/>) (Jain *et al.*, 2009; The UniProt Consortium, 2011). The occurrence of the GO terms (76 biological processes) of the proteins was counted with the CateGORizer web tool in the "MGI_GO_slim2" ancestor terms using the multiple count method (<http://www.animalgenome.org/tools/catego/>) (Hu *et al.*, 2008). UniProtKB ACs of the proteins were queried against the KEGG PATHWAY for *Rattus norvegicus* with the KEGG Mapper on the GenomeNet web site (<http://www.genome.jp/en/>).

RESULTS

Effects of ethanol on the growth of cultured rat embryos

Ethanol inhibited the growth of cultured embryos at concentrations of 130 mM or higher in a concentration-dependent manner (Table 1). Deformed organs included branchial arch, heart, neural tube, optic vesicle, otic vesicle, somite, and tail (Fig. 1), which is in agreement with previous reports (Giavini *et al.*, 1992; Zhou *et al.*, 2011).

Compared to blood ethanol levels found in humans, these embryotoxic ethanol concentrations are rather high; however, an ethanol concentration of 150 mM can be observed after acute alcohol intake in chronic alcoholics and 200 mM of ethanol has often been used in *in vitro* toxicological experiments (Li and Kim, 2003; Szabo *et al.*, 1994; Wentzel and Eriksson, 2008).

Effects of ethanol on embryonic protein expression

About 900 protein spots were matched through sixteen 2-DE gels (four gels per experimental group). Quality changes, i.e., appearance or disappearance, in the

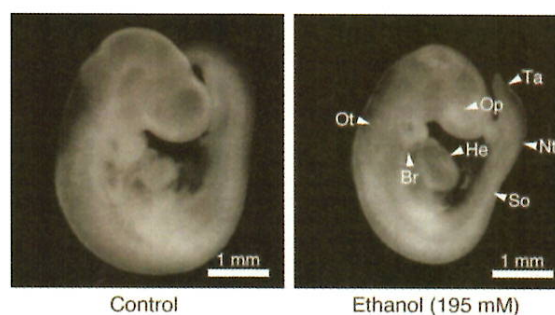


Fig. 1. Appearance of rat embryos cultured in the presence of ethanol. Rat embryos at the end of 24-hr culture are shown after removal of the embryonic membranes. Arrowheads indicate deformed organs. Br, branchial arch; He, heart; Nt, neural tube; Op, optic vesicle; Ot, otic vesicle; So, somite; Ta, tail.

Table 1. Growth of day 10.5 rat embryos cultured in the presence of ethanol

	Ethanol (mM)			
	0 (Control)	65	130	195
No. of embryos	6	5	6	5
No. of viable embryos	6 (100%)	5 (100%)	6 (100%)	5 (100%)
Crown-rump length (mm)	4.11 ± 0.15	3.99 ± 0.17	3.72 ± 0.29*	3.25 ± 0.28**
Head length (mm)	2.23 ± 0.11	2.16 ± 0.14	2.01 ± 0.22	1.74 ± 0.35**
No. of somite pairs	26.7 ± 0.52	26.4 ± 0.55	24.5 ± 2.81	21.2 ± 2.49**
No. of embryos with deformed organ	0	0	3 (50%)	5 (100%)**
Branchial arch	0	0	2 (33%)	4 (80%)*
Heart	0	0	1 (17%)	3 (60%)
Neural tube	0	0	2 (33%)	2 (40%)
Optic vesicle	0	0	2 (33%)	5 (100%)**
Otic vesicle	0	0	2 (33%)	5 (100%)**
Somite	0	0	3 (50%)	5 (100%)**
Tail	0	0	2 (33%)	4 (80%)*

Embryos were cultured for 24 hr by the roller method. Asterisks indicate statistically significant differences compared to the control group identified by Dunnett's multiple comparison test or Fisher's exact test (* $p < 0.05$; ** $p < 0.01$).

Proteomics of ethanol embryotoxicity

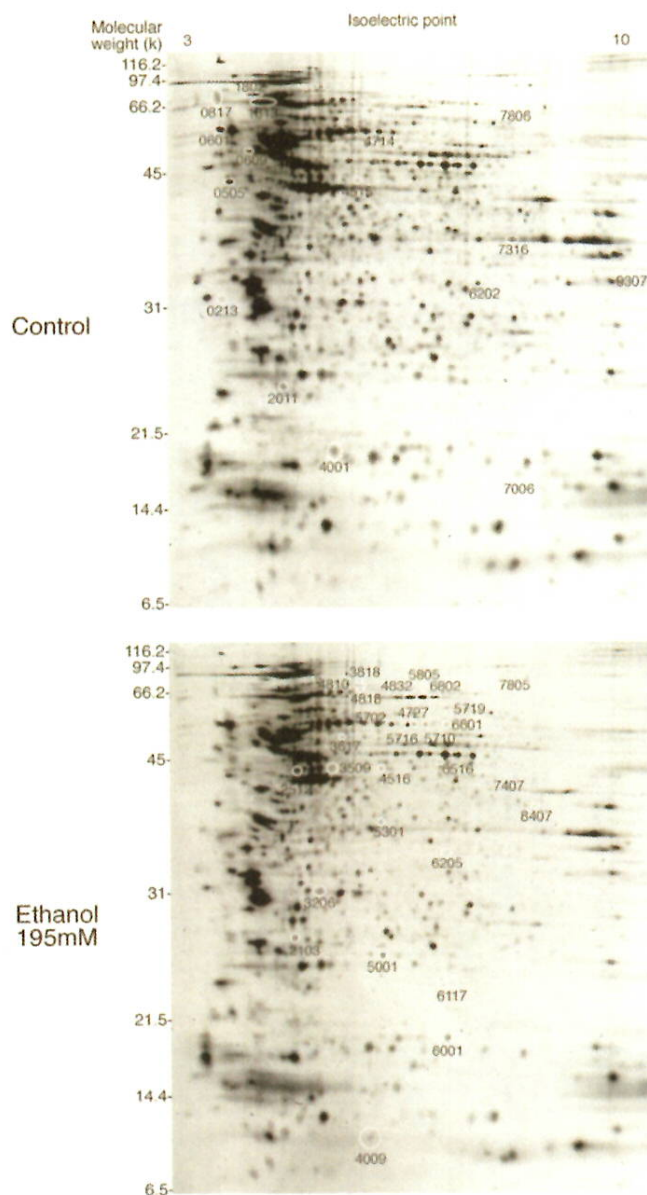


Fig. 2. Two-dimensional electrophoresis pattern of proteins from rat embryos cultured in the presence of ethanol. Representative gels are shown for the control and ethanol (195 mM) groups. Proteins with ethanol-induced expression changes are indicated by circles with standard spot numbers (SSPs); decreased proteins are indicated in the "control" gel (top) and increased ones in the "ethanol" gel (bottom).

protein spots were not observed. Ethanol-induced quantitative changes were noted in 44 spots, i.e., 16 spots were decreased and 28 spots were increased by 1.5-fold or more. The differences between the 195 mM ethanol group and the control group were significant and occurred for

most proteins in a concentration-dependent manner (Figs. 2 and 3). Of these spots, 23 were analyzed by MS, resulting in the identification of 7 proteins that were decreased (Table 2) and 11 proteins that were increased (Table 3). Some proteins that were increased, e.g., alpha-fetopro-

Table 2. Proteins whose expression was decreased and their GO terms identified by two-dimensional electrophoresis analysis of rat embryos cultured in the presence of ethanol

SSP	Protein Name	UniProtKB AC	GO term for Biological Process
0505	Protein SET	Q63945	GO:0006334 nucleosome assembly
0601	Nucleosome assembly protein 1-like 1	Q972G8	GO:0006334 nucleosome assembly
0817	Myristoylated alanine-rich C-kinase substrate	P30009	n.a.
1802	78 kDa glucose-regulated protein	P06761	GO:0006916 anti-apoptosis GO:0006983 ER overload response GO:0006987 activation of signaling protein activity involved in unfolded protein response GO:0021589 cerebellum structural organization GO:0021680 cerebellar Purkinje cell layer development GO:0030512 negative regulation of transforming growth factor beta receptor signaling pathway GO:0031398 positive regulation of protein ubiquitination GO:0042149 cellular response to glucose starvation GO:0043066 negative regulation of apoptotic process GO:0043154 negative regulation of cysteine-type endopeptidase activity involved in apoptotic process GO:0051603 proteolysis involved in cellular protein catabolic process GO:0006351 transcription, DNA-dependent GO:0006355 regulation of transcription, DNA-dependent GO:0006950 response to stress GO:0045892 negative regulation of transcription, DNA-dependent GO:0051085 chaperone mediated protein folding requiring cofactor GO:0061077 chaperone-mediated protein folding
1813	Heat shock cognate 71 kDa protein	P63018	n.a.
2011	Uncharacterized protein	D3ZRS6	n.a.
4714	Protein disulfide-isomerase A3	P11598	GO:0006662 glycerol ether metabolic process GO:0043065 positive regulation of apoptotic process GO:0045454 cell redox homeostasis

n.a., not available.

Table 3. Proteins whose expression was increased and their GO terms identified by two-dimensional electrophoresis analysis of rat embryos cultured in the presence of ethanol

SSP	Protein Name	UniProtKB AC	GO term for Biological Process
2103	Myosin light chain 3	P16409	GO:0002026 regulation of the force of heart contraction GO:0006936 muscle contraction GO:0006942 regulation of striated muscle contraction GO:0007519 skeletal muscle tissue development GO:0055010 ventricular cardiac muscle tissue morphogenesis GO:0060048 cardiac muscle contraction
2512	BWK4 AND Eukaryotic initiation factor 4A-II OR Eukaryotic translation initiation factor 4A1	Q5VLR5 AND Q5RK11 OR Q6P3V8	GO:0006457 protein folding GO:0006950 response to stress GO:0006986 response to unfolded protein GO:0009100 glycoprotein metabolic process GO:0045454 cell redox homeostasis AND GO:0006413 translational initiation

3509	Eukaryotic translation initiation factor 4A1	Q6P3V8	GO:0006413 translational initiation
4009	Fatty acid-binding protein	P07483	GO:0006631 fatty acid metabolic process GO:0006635 fatty acid beta-oxidation GO:0006656 phosphatidylcholine biosynthetic process GO:0006810 transport GO:0015909 long-chain fatty acid transport GO:0032868 response to insulin stimulus GO:0042493 response to drug GO:0070542 response to fatty acid
5001	Adenine phosphoribosyltransferase	P36972	GO:0006166 purine ribonucleoside salvage GO:0006168 adenine salvage GO:0007595 lactation
6001	Cofilin-1	P45592	GO:0009116 nucleoside metabolic process GO:0032869 cellular response to insulin stimulus GO:0006606 protein import into nucleus GO:0007010 cytoskeleton organization GO:0022604 regulation of cell morphogenesis GO:0030030 cell projection organization GO:0045792 negative regulation of cell size
6516	Elongation factor 1-gamma	Q68FR6	GO:0006412 translation GO:0006414 translational elongation
4727	Protein disulfide-isomerase A3	P11598	GO:0006662 glycerol ether metabolic process GO:0043065 positive regulation of apoptotic process GO:0045454 cell redox homeostasis
5702			
5710			
5716			
6601			
4810	Alpha-fetoprotein	P02773	GO:0001542 ovulation from ovarian follicle GO:0001889 liver development GO:0006810 transport GO:0010033 response to organic substance GO:0019953 sexual reproduction GO:0031016 pancreas development GO:0031100 organ regeneration GO:0042448 progesterone metabolic process GO:0060395 SMAD protein signal transduction
4818			
4832	Serum albumin	P02770	GO:0006810 transport GO:0006950 response to stress GO:0007584 response to nutrient GO:0009267 cellular response to starvation GO:0010033 response to organic substance GO:0019836 hemolysis by symbiont of host erythrocytes GO:0042311 vasodilation GO:0043066 negative regulation of apoptotic process GO:0046010 positive regulation of circadian sleep wake cycle, non-REM sleep GO:0046689 response to mercury ion GO:0051659 maintenance of mitochondrion location GO:0070541 response to platinum ion
5805			
6802			

SSP 2512 contained two proteins.

Table 4. KEGG pathway mapping of proteins identified by two-dimensional electrophoresis analysis of rat embryos cultured in the presence of ethanol

Pathway ID	Pathway name	UniProtKB AC	Protein Name (Total number of mapped pathways)
mo04612	Antigen processing and presentation	P06761	78 kDa glucose-regulated protein (4)
		P11598	Protein disulfide-isomerase A3 (2)
		P63018	Heat shock cognate 71 kDa protein (9)
mo04141	Protein processing in endoplasmic reticulum	P06761	78 kDa glucose-regulated protein (4)
mo04141	Protein processing in endoplasmic reticulum	P11598	Protein disulfide-isomerase A3 (2)
		P63018	Heat shock cognate 71 kDa protein (9)
		P63018	Heat shock cognate 71 kDa protein (9)
mo05134	Legionellosis	P63018	Heat shock cognate 71 kDa protein (9)
		Q68FR6	Elongation factor 1-gamma (1)
mo03040	Spliceosome	P63018	Heat shock cognate 71 kDa protein (9)
mo04010	MAPK signaling pathway	P63018	Heat shock cognate 71 kDa protein (9)
mo04144	Endocytosis	P63018	Heat shock cognate 71 kDa protein (9)
mo05145	Toxoplasmosis	P63018	Heat shock cognate 71 kDa protein (9)
mo05162	Measles	P63018	Heat shock cognate 71 kDa protein (9)
mo05164	Influenza A	P63018	Heat shock cognate 71 kDa protein (9)
mo04360	Axon guidance	P45592	Cofilin-1 (4)
mo04666	Fe gamma R-mediated phagocytosis	P45592	Cofilin-1 (4)
mo04810	Regulation of actin cytoskeleton	P45592	Cofilin-1 (4)
mo05133	Pertussis	P45592	Cofilin-1 (4)
mo04260	Cardiac muscle contraction	P16409	Myosin light chain 3 (3)
mo05410	Hypertrophic cardiomyopathy (HCM)	P16409	Myosin light chain 3 (3)
mo05414	Dilated cardiomyopathy	P16409	Myosin light chain 3 (3)
mo00230	Purine metabolism	P36972	Adenine phosphoribosyltransferase (2)
mo01100	Metabolic pathways	P36972	Adenine phosphoribosyltransferase (2)
mo03060	Protein export	P06761	78 kDa glucose-regulated protein (4)
mo05020	Prion diseases	P06761	78 kDa glucose-regulated protein (4)
mo03013	RNA transport	Q5RKL1	Eukaryotic initiation factor 4A-II (1)
		OR	OR
mo03320	PPAR signaling pathway	Q6P3V8	Eukaryotic translation initiation factor 4A1 (1)
		P07483	Fatty acid-binding protein (1)

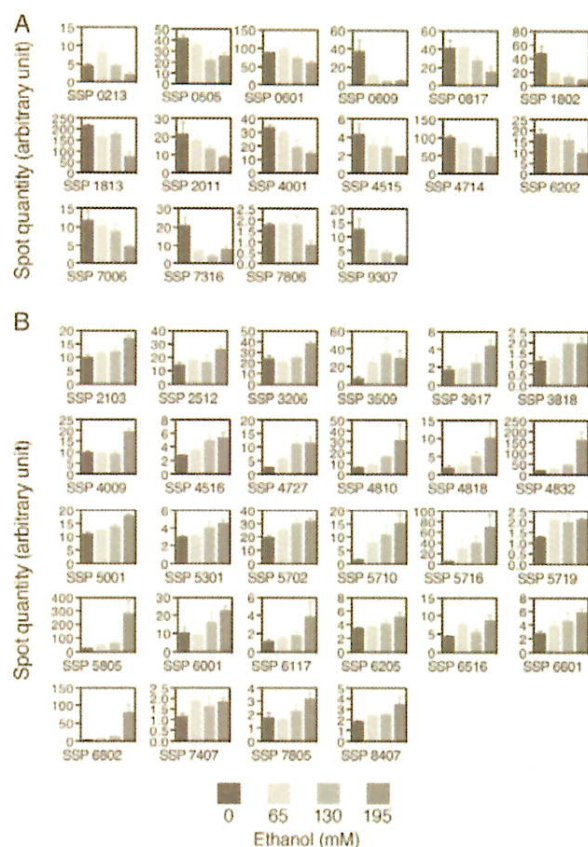


Fig. 3. Quantification of protein spots with expression changes in two-dimensional electrophoresis gels from rat embryos cultured in the presence of ethanol. Intensities of protein spots with ethanol-induced expression changes are shown. A. Protein spots with decreased intensity. B. Protein spots with increased intensity. Error bars indicate the standard error of the mean.

tein (standard spot numbers (SSPs) 4810, 4818), cofilin-1 (SSP 6001), and serum albumin (SSPs 4832, 5805, 6802), were the same as those identified as candidate proteins involved in embryotoxicity in our previous studies (Usami *et al.*, 2009, 2008); cofilin-1, which was increased, was found to be in its phosphorylated form.

Several protein spots were identified as charge variant forms of the same proteins, i.e., protein disulfide isomerase A3 (PDIA3; SSPs 4714, 4727, 5702, 5710, 5716, 6601), alpha-fetoprotein (SSPs 4810, 4818), and serum albumin (SSPs 4832, 5805, 6802). The quantities of spots that were identified as PDIA3 were increased (SSPs 4727,

5702, 5710, 5716, 6601), as well as decreased (SSP 4714) (Fig. 3). Because the PDIA3 spot with decreased quantity was the most acidic spot, it appeared that a basic pI shift of PDIA3 occurred in the groups exposed to ethanol.

Classification and mapping of proteins with ethanol-induced expression changes

According to their GO terms, the identified proteins were classified into various categories; the six major categories were “metabolism” (including 32% of the GO terms), “protein metabolism” (13%), “death” (9%), “developmental processes” (9%), “cell organization and biogenesis” (8%), and “stress response” (8%).

The identified proteins were mapped to 22 pathways using the KEGG pathway mapper (Table 4). Multiple proteins, i.e., PDIA3, 78-kDa glucose-regulated protein (SSP 1802), and heat shock cognate 71-kDa protein (SSP 1813), were mapped to the same two pathways, i.e., “protein processing in endoplasmic reticulum” (rno04141) and “antigen processing and presentation” (rno04612). Some proteins were mapped to multiple pathways, e.g., heat shock cognate 71-kDa protein (nine pathways), 78-kDa glucose-regulated protein (four pathways), and cofilin-1 (four pathways).

DISCUSSION

As mechanisms of ethanol-induced embryotoxicity, oxidative stress, and inhibited retinoid synthesis have been proposed (Goodlett *et al.*, 2005), which seems to be in accordance with the GO classification (32% metabolism and 8% stress response) of the proteins identified in the present study. In this context, expression changes in PDIA3 (also known as GRp58 and ERp57) are intriguing because it is an endoplasmic reticulum stress protein with oxidoreductase activity that regulates cellular redox homeostasis (Frickel *et al.*, 2004; Ni and Lee, 2007). PDIA3 is also involved in the nuclear translocation of retinoic acid receptor alpha (Zhu *et al.*, 2010) and its deficiency is embryonic lethal (Coe *et al.*, 2010). The identified proteins with GO terms classified into “death” may be involved in ethanol-induced apoptosis of neuronal cells, which has frequently been observed (Ahlgren *et al.*, 2002; Giles *et al.*, 2008). The present results also agreed with some biological networks that were perturbed by ethanol in cultured whole mouse embryos, involving cell death, reproductive system and antigen processing (Mason *et al.*, 2012). The pathways associated with multiple identified proteins may be more susceptible to ethanol, because these pathways could be affected at multiple steps simultaneously. On the other hand, the finding that

multiple pathways were associated with the same proteins might partially explain the complexity of ethanol-induced embryotoxicity.

ACKNOWLEDGMENT

This work was supported by a Health and Labor Science Research Grant from the Ministry of Health, Labor and Welfare in Japan.

REFERENCES

- Ahlgren, S.C., Thakur, V. and Bronner-Fraser, M. (2002): Sonic hedgehog rescues cranial neural crest from cell death induced by ethanol exposure. *Proc. Natl. Acad. Sci. USA*, **99**, 10476-10481.
- Chen, H., Boontheung, P., Loo, R.R., Xie, Y., Loo, J.A., Rao, J.Y. and Collins, M.D. (2008): Proteomic analysis to characterize differential mouse strain sensitivity to cadmium-induced forelimb teratogenesis. *Birth Defects Res. A Clin. Mol. Teratol.*, **82**, 187-199.
- Coe, H., Jung, J., Groenendyk, J., Prins, D. and Michalak, M. (2010): ERp57 modulates STAT3 signaling from the lumen of the endoplasmic reticulum. *J. Biol. Chem.*, **285**, 6725-6738.
- Frickel, E.-M., Frei, P., Bouvier, M., Stafford, W.F., Helenius, A., Glockshuber, R. and Ellgaard, L. (2004): ERp57 is a multifunctional thiol-disulfide oxidoreductase. *J. Biol. Chem.*, **279**, 18277-18287.
- Giavini, E., Brocchia, M.L., Prati, M., Bellomo, D. and Menegola, E. (1992): Effects of ethanol and acetaldehyde on rat embryos developing *in vitro*. *Vitr. Cell. Dev. Biol.*, **28A**, 205-210.
- Giles, S., Boehm, P., Brogan, C. and Bannigan, J. (2008): The effects of ethanol on CNS development in the chick embryo. *Reprod. Toxicol.*, **25**, 224-230.
- Goodlett, C.R., Horn, K.H. and Zhou, F.C. (2005): Alcohol teratogenesis: mechanisms of damage and strategies for intervention. *Exp. Biol. Med.*, **230**, 394-406.
- Groebe, K., Hayess, K., Klemm-Manns, M., Schwall, G., Wozny, W., Steemans, M., Peters, A.K., Sastri, C., Jaeckel, P., Stegmann, W., Zengerling, H., Schopf, R., Poznanovic, S., Stummann, T.C., Seiler, A., Spielmann, H. and Schratzenholz, A. (2010): Protein biomarkers for *in vitro* testing of embryotoxicity. *J. Proteome Res.*, **9**, 5727-5738.
- Hu, Z.-L., Bao, J. and Reecy, J.M. (2008): CateGORizer: A web-based program to batch analyze gene ontology classification categories. *Online J. Bioinforma.*, **9**, 108-112.
- Jain, E., Bairoch, A., Duvaud, S., Phan, I., Redaschi, N., Suzek, B.E., Martin, M.J., McGarvey, P. and Gasteiger, E. (2009): Infrastructure for the life sciences: design and implementation of the UniProt website. *BMC Bioinformatics*, **10**, 136.
- Li, H. and Kim, K.H. (2003): Effects of ethanol on embryonic and neonatal rat testes in organ cultures. *J. Androl.*, **24**, 653-660.
- Mason, S., Anthony, B., Lai, X., Ringham, H.N., Wang, M., Witzmann, F.A., You, J.-S. and Zhou, F.C. (2012): Ethanol exposure alters protein expression in a mouse model of fetal alcohol spectrum disorders. *Int. J. Proteomics*, **2012**, 867141.
- Ni, M. and Lee, A.S. (2007): ER chaperones in mammalian development and human diseases. *FEBS Lett.*, **581**, 3641-3651.
- Szabo, G., Puppulo, M., Verma, B. and Catalano, D. (1994): Regulatory potential of ethanol and retinoic acid on human monocyte functions. *Alcohol. Clin. Exp. Res.*, **18**, 548-554.
- UniProt Consortium (2011): Ongoing and future developments at the Universal Protein Resource. *Nucleic Acids Res.*, **39**, D214-219.
- Usami, M. and Mitsunaga, K. (2011): Proteomic analysis and *in vitro* developmental toxicity tests for mechanism-based safety evaluation of chemicals. *Expert Rev. Proteomics*, **8**, 153-155.
- Usami, M., Mitsunaga, K., Nakazawa, K. and Doi, O. (2008): Proteomic analysis of selenium embryotoxicity in cultured post-implantation rat embryos. *Birth Defects Res. B Dev. Reprod. Toxicol.*, **83**, 80-96.
- Usami, M., Nakajima, M., Mitsunaga, K., Miyajima, A., Sunouchi, M. and Doi, O. (2009): Proteomic analysis of indium embryotoxicity in cultured postimplantation rat embryos. *Reprod. Toxicol.*, **28**, 477-488.
- Wentzel, P. and Eriksson, U.J. (2008): Genetic influence on dysmorphogenesis in embryos from different rat strains exposed to ethanol *in vivo* and *in vitro*. *Alcohol. Clin. Exp. Res.*, **32**, 874-887.
- Zhou, F.C., Zhao, Q., Liu, Y., Goodlett, C.R., Liang, T., McClintick, J.N., Edenberg, H.J. and Li, L. (2011): Alteration of gene expression by alcohol exposure at early neurulation. *BMC Genomics*, **12**, 124.
- Zhu, L., Santos, N.C. and Kim, K.H. (2010): Disulfide isomerase glucose-regulated protein 58 is required for the nuclear localization and degradation of retinoic acid receptor alpha. *Reproduction*, **139**, 717-731.

Title

Effects of 13 developmentally toxic chemicals on the migration of rat cephalic neural crest cells in vitro

First author's surname

Usami

Short title

Chemical effects on neural crest cells

Names of authors

Makoto Usami¹, Katsuyoshi Mitsunaga², Atsuko Miyajima³, Mina Takamatu⁴, Shugo Kazama⁴, Tomohiko Irie¹, Osamu Doi⁵, Tatsuya Takizawa⁴

Affiliation

¹Division of Pharmacology, National Institute of Health Sciences, Tokyo 158-8501,

²School of Pharmaceutical Sciences, Toho University, Chiba 274-8510, ³Division of

Medical Devices, National Institute of Health Sciences, Tokyo 158-8501, ⁴School of

Veterinary Medicine, Azabu University, Kanagawa 252-5201, ⁵United Graduate School of Agricultural Science, Gifu University, Gifu 501-1193.

Corresponding author

Makoto Usami, Ph.D.

Division of Pharmacology, National Institute of Health Sciences,

1-18-1, Kamiyoga, Setagaya, Tokyo 158-8501, Japan

Tel: +81-3-3700-1141(ext.342); Fax: +81-3-3707-6950

E-mail: usami@nihs.go.jp

This article has been accepted for publication and undergone full peer review but has not been through the copyediting, typesetting, pagination and proofreading process, which may lead to differences between this version and the Version of Record. Please cite this article as doi: 10.1111/cga.12121

1/28

This article is protected by copyright. All rights reserved.

ABSTRACT

The inhibition of neural crest cell (NCC) migration has been considered as a possible pathogenic mechanism underlying chemical developmental toxicity. In this study, we examined the effects of 13 developmentally toxic chemicals on the migration of rat cephalic NCCs (cNCCs) by using a simple in vitro assay. cNCCs were cultured for 48 h as emigrants from rhombencephalic neural tubes explanted from rat embryos at day 10.5 of gestation. The chemicals were added to the culture medium at 24h of culture.

Migration of cNCCs was measured as the change in the radius (radius ratio) calculated from the circular spread of cNCCs between 24 and 48 h of culture. Of the chemicals examined, 13-*cis*-retinoic acid, ethanol, ibuprofen, lead acetate, salicylic acid, and selenate inhibited the migration of cNCCs at their embryotoxic concentrations; no effects were observed for acetaminophen, caffeine, indium, phenytoin, selenite, tributyltin, and valproic acid. In a cNCC proliferation assay, ethanol, ibuprofen, salicylic acid, selenate, and tributyltin inhibited cell proliferation, suggesting the contribution of the reduced cell number to the inhibited migration of cNCCs. It was determined that several developmentally toxic chemicals inhibited the migration of cNCCs, the effects of which were manifested as various craniofacial abnormalities.

Key words

Developmental toxicity; Embryo; Migration assay; Neural crest cell; Rat

INTRODUCTION

In vertebrate embryos, neural crest cells (NCCs) migrate to various tissues throughout the body and contribute to tissue organization; malfunction NCCs can lead to dysmorphologies, tumors and syndromes called neurocristopathies (Hall 2009; Le Douarin & Kalcheim 1999). The inhibition of NCC migration has, therefore, been considered as a possible pathogenic mechanism underlying chemical developmental toxicity. It has been shown, for example, that all-*trans*-retinoic acid, a well-known teratogen, inhibits the migration of cephalic NCCs (cNCCs), causing branchial abnormalities in cultured mouse and rat embryos (Menegola et al. 2004).

The effects of chemicals on the migration of NCCs in mammals, however, have not been fully investigated, probably because no convenient experimental methods are available. The migration of NCCs has been examined by time-lapse video image analysis of fluorescence-labeled cells (Fuller et al. 2002; Kawakami et al. 2011), or by human neural crest stem cells with scratch assay (Zimmer et al. 2012). These methods are complicated and therefore not ideal for testing of chemicals in a common toxicity laboratory.

Recently, we established a simple in vitro assay that enabled examination of the effects of chemicals on the migration of cNCCs and trunk NCCs (tNCCs) (Usami et al. 2014b). In this method, NCCs are cultured as emigrants from isolated neural tubes of day 10.5 rat embryos. The cultured NCCs are exposed to test chemicals and their migration is determined as the radius ratio calculated from circular spread of the NCCs during the exposure period. Using this method we examined the effects of 13 developmentally toxic chemicals on the migration of cNCCs. We also examined the effects of chemicals on the proliferation of cNCCs, because this migration assay depends on the spread of cells and

can therefore be influenced by the cell number.

We selected developmentally toxic chemicals on the basis of our interest in our related study such as proteomics of embryos (Usami et al. 2014a; Usami et al. 2009; Usami et al. 2008) and metabolomics of hepatocytes (Kim et al. 2014) since there was little information about the effects of chemicals on the migration of cNCCs. However, we considered that the chemicals include both ones might affect cNCC migration, e.g., ethanol, and selenate, and ones might not, e.g., indium, and tributyltin, which was speculated from their potential to cause craniofacial abnormality.

MATERIALS AND METHODS

Animals

Wistar rats (Crj: WI, Charles River Japan Inc., Kanagawa, Japan) were used. Pregnant rats were obtained by mating female and male rats overnight, and the plug day was designated as day 0.5 of gestation. All the animal experiments were performed according to the guidelines for animal experiments of the National Institute of Health Sciences.

Chemicals

Acetaminophen (CAS 103-90-2), 13-*cis*-retinoic acid (CAS 4759-48-2), ibuprofen (CAS 31121-93-4), salicylic acid (CAS 54-21-7), selenate (CAS 13410-01-0), and selenite (CAS 10102-18-8) were purchased from Sigma-Aldrich Co. (St. Louis, MO).

Caffeine (CAS 58-08-2), ethanol (CAS 64-17-5), indium (CAS 22519-64-8), lead acetate (CAS 6080-56-4), phenytoin (CAS 57-41-0), and tributyltin (CAS 1461-22-9) were purchased from Wako Pure Chemical Industries (Osaka, Japan). Valproic acid (CAS 1069-66-5) was purchased from Merck Co. (Darmstadt, Germany).

Culture of NCCs

Rat NCCs were cultured as emigrated cells from neural tubes of rat embryos at day 10.5 of gestation as previously described (Usami et al. 2014b), according to the culture schedule shown in Fig. 1. Neural tubes were excised from the rhombencephalic (for cNCCs) or trunk (for tNCCs) region of the embryos in Hanks' balanced salt solution with sharpened tungsten needles. The excised neural tubes were cultured in 35-mm culture dishes (BD Primaria; Becton, Dickinson and Company, Franklin Lakes, NJ) containing 2 ml of Dulbecco's Modified Eagle Medium with high glucose (DMEM; GIBCO, Life

Technologies Corp., Carlsbad, CA) and 10% (v/v) fetal bovine serum (GIBCO) at 37°C with 5% CO₂ for 48 h.

Phase-contrast images of cultured NCCs were recorded digitally at a magnification of ×10 with a microscope at 24 and 48 h of culture (BZ-9000; Keyence, Osaka, Japan). In the proliferation assay, the neural tube was removed at 18 h of culture, and the cell nuclei were stained with 4',6-diaminodino-2-phenylindole (DAPI, Invitrogen) and fluorescent images were photographed with the microscope at 48 h of culture. Representative photographs of the cNCCs are shown in Fig. 2.

Addition of chemicals

The chemicals were added at 24 h of culture by replacing the culture medium. For addition to the culture medium, caffeine, ethanol, salicylic acid, selenate, selenite, and valproic acid were directly dissolved in or diluted with the culture medium.

Acetaminophen, 13-*cis*-retinoic acid, phenytoin, and tributyltin were dissolved in or diluted with dimethyl sulfoxide and 5 µl each of the solutions was added to 5 ml of the culture medium. Ibuprofen, indium, and lead acetate were dissolved in pure water and 100 µl each of the solutions was added to 4.9 ml of the culture medium.

The concentrations of the following chemicals in the culture medium were their embryotoxic concentrations obtained from the literature: acetaminophen (Weeks et al. 1990), caffeine (Robinson et al. 2010; Shreiner et al. 1986), 13-*cis*-retinoic acid (Lee et al. 1991), ethanol (Usami et al. 2014a), ibuprofen (Guest et al. 1994), indium (Usami et al. 2009), lead acetate (Zhao et al. 1997), phenytoin (Winn 2002), salicylic acid (Greenaway et al. 1985), selenate (Usami et al. 2008), selenite (Usami et al. 2008), tributyltin (Cooke et al. 2008; Adeeko et al. 2003), and valproic acid (Guest et al. 1994)

Migration assay of NCCs

The migration distance of NCCs was calculated as the increased radius of the circular spread of NCCs that emigrated from the neural tubes between 24 and 48 h of culture (Usami et al. 2014b). The outermost NCCs in each of the cultured neural tubes were connected with the polygon tool as if a rubber band were put around the cells, and its inner area was measured as a pixel count. Considering the polygon as a circle, its radius ratio was calculated: $\text{radius ratio} = (\text{radius at 48 h} - \text{radius at 24 h}) / \text{radius at 24 h}$. This ratio was then normalized as a percent of the simultaneous control to express the NCC migration for comparisons among experiments.

Proliferation assay for NCCs

NCC proliferation was evaluated as a ratio of the cell count at 48 h to that at 24 h of culture, and the effects of chemicals were examined. The cells were counted manually at 24 h on the phase-contrast image with the Cell Counter plugin of the ImageJ software (<http://rsb.info.nih.gov/ij/>, 1997–2009; Rasband, W.S., ImageJ, U. S. National Institutes of Health, Bethesda, MD, USA). The cell count at 48 h was estimated as the count of stained cell nuclei from the fluorescence image with the Hybrid Cell Count function of the BZ-X Analyzer software (Keyence). The average cell counts in an intact control group were 170.6 at 24 h and 272.1 at 48 h (n = 10). Two proliferation indices, the cell count ratio and the cell proliferation ratio, were calculated as follows: $\text{cell count ratio} = \text{cell count at 48 h} / \text{cell count at 24 h}$, and $\text{cell proliferation ratio} = (\text{cell count at 48 h} - \text{cell count at 24 h}) / \text{cell count at 24 h}$.

Although these indices are basically the same, the latter is more suitable for representing

the proliferation rate and the former is more useful for comparison with the migration index. These indices were normalized to the control to allow for comparisons among experiments.

Statistical analysis

Statistical significance of the difference between the experimental groups was examined by the Student *t* test at a probability level of 5%.